AGU PUBLICATIONS

JGR

Journal of Geophysical Research: Oceans

RESEARCH ARTICLE

10.1002/2015JC011202

Key Points:
- Inherent optical properties (IOPs) are characterized in a optically complex lake
- IOP-constituent relationships vary markedly from those in ocean waters
- Variability of specific IOPs has implications for retrievals from remote sensing

Correspondence to:
C. A. L. Riddick,
c.a.riddick@stir.ac.uk

Citation:
Riddick, C. A. L., P. D. Hunter, A. N. Tyler, V. Martinez-Vicente, H. Horváth, A. W. Kovács, L. Vörös, T. Preston, and M. Présing (2015), Spatial variability of absorption coefficients over a biogeochemical gradient in a large and optically complex shallow lake, *J. Geophys. Res. Oceans*, *120*, 7040–7066, doi:10.1002/2015JC011202.

Received 5 AUG 2015
Accepted 6 OCT 2015
Accepted article online 8 OCT 2015
Published online 31 OCT 2015

Spatial variability of absorption coefficients over a biogeochemical gradient in a large and optically complex shallow lake

Caitlin A. L. Riddick[1], Peter D. Hunter[1], Andrew N. Tyler[1], Victor Martinez-Vicente[2], Hajnalka Horváth[3], Attila W. Kovács[3], Lajos Vörös[3], Tom Preston[4], and Mátyás Présing[3,5]

[1]Biological and Environmental Sciences, School of Natural Sciences, University of Stirling, Stirling, UK, [2]Plymouth Marine Laboratory, Plymouth, UK, [3]Balaton Limnological Institute, MTA Centre for Ecological Research, Tihany, Hungary, [4]Stable Isotope Biochemistry Lab, Scottish Universities Environmental Research Centre, East Kilbride, UK, [5]Deceased 17 June 2015

Abstract In order to improve robustness of remote sensing algorithms for lakes, it is vital to understand the variability of inherent optical properties (IOPs) and their mass-specific representations (SIOPs). In this study, absorption coefficients for particulate and dissolved constituents were measured at 38 stations distributed over a biogeochemical gradient in Lake Balaton, Hungary. There was a large range of phytoplankton absorption ($a_{ph}(\lambda)$) over blue and red wavelengths ($a_{ph}(440) = 0.11–4.39\ m^{-1}$, $a_{ph}(675) = 0.048–2.52\ m^{-1}$), while there was less variability in chlorophyll-specific phytoplankton absorption ($a^*_{ph}(\lambda)$) in the lake ($a^*_{ph}(440) = 0.022 \pm 0.0046\ m^2\ mg^{-1}$, $a^*_{ph}(675) = 0.010 \pm 0.0020\ m^2\ mg^{-1}$) and adjoining wetland system, Kis-Balaton ($a^*_{ph}(440) = 0.017 \pm 0.0015\ m^2\ mg^{-1}$, $a^*_{ph}(675) = 0.0088 \pm 0.0017\ m^2\ mg^{-1}$). However, in the UV, $a^*_{ph}(350)$ significantly increased with increasing distance from the main inflow (Zala River). This was likely due to variable production of photoprotective pigments (e.g., MAAs) in response to the decreasing gradient of colored dissolved organic matter (CDOM). The slope of CDOM absorption (S_{CDOM}) also increased from west to east due to larger terrestrial CDOM input in the western basins. Absorption by nonalgal particles ($a_{NAP}(\lambda)$) was highly influenced by inorganic particulates, as a result of the largely mineral sediments in Balaton. The relative contributions to the absorption budget varied more widely than oceans with a greater contribution from NAP (up to 30%), and wind speed affected the proportion attributed to NAP, phytoplankton, or CDOM. Ultimately, these data provide knowledge of the heterogeneity of (S)IOPs in Lake Balaton, suggesting the full range of variability must be considered for future improvement of analytical algorithms for constituent retrieval in inland waters.

1. Introduction

Understanding the sources and magnitude of variability in light absorption in lakes and reservoirs is fundamentally important to studies concerned with photochemistry [*Moran and Zepp*, 1997; *Bertilsson and Tranvik*, 2000], photosynthesis [*Blache et al*., 2011], primary production [*Tilstone et al*., 2005; *Lee et al*., 2011], heat and energy transfers [*Jolliff et al*., 2008; *Dera and Wozniak*, 2010], and biogeochemical models [*Ciavatta et al*., 2014]. The absorption and scattering of light (termed inherent optical properties, IOPs) are also key processes influencing the magnitude and spectral distribution of the water-leaving reflectance signal measured by Earth-observing satellites [*Mobley*, 1994; *Kirk*, 1994]. Remote sensing has allowed for characterization of water bodies at improved spatial and temporal scales with the aim of monitoring water quality operationally in ocean, coastal and, more recently, inland waters. However, remote sensing algorithms developed for retrieval of physical and biogeochemical properties in open ocean waters are often inaccurate when applied to more turbid and optically complex inland waters [*Sathyendranath et al*., 1999; *IOCCG*, 2000; *Binding et al*., 2008]. Inland waters typically have higher concentrations of phytoplankton biomass, detritus, inorganic particulates and color dissolved organic matter (CDOM), and large percentages of suspended particulates can be land derived. Moreover, the biogeochemical properties of inland waters do not covary over space and time, resulting in potentially large variability in the IOPs of the optically active constituents (OACs) [*Binding et al*., 2008; *Palmer et al*., 2015]. In order to improve the performance of algorithms for the retrieval of biogeochemical parameters in lakes, it is vital that we develop a better understanding of the variability in the absorption and backscattering coefficients ($a(\lambda)$ and $b_b(\lambda)$; m^{-1}) of the main OACs in

lakes (i.e., phytoplankton, nonalgal particles (NAP), and colored dissolved organic matter (CDOM)) and their mass-specific representations ($a^*(\lambda)$ and $b_b^*(\lambda)$; $m^2\ mg^{-1}$). When light enters the water column photons are removed from its path by absorption, and $a(\lambda)$ is defined as the sum of absorption by particulate and dissolved constituents and water itself. Light is also scattered by suspended particles, and the scattering coefficient ($b(\lambda)$) is commonly defined as a measure of the total magnitude of scattered light (without regard to its angular distribution). $b_b(\lambda)$ can therefore be defined as the total light scattered in the backward direction. The sum of $a(\lambda)$ and $b(\lambda)$ is the beam attenuation coefficient ($c(\lambda)$), or the total light attenuated in the water column. Knowledge of the IOPs is particularly important for radiative transfer studies and the development of analytically based inversion algorithms. The bio-optical properties of open ocean [*Morel and Maritorena*, 2001] and coastal waters [*Babin et al*., 2003b] have been extensively studied over the last four decades, but our knowledge of these properties in lakes and other inland waters remains comparatively poor [*Luis Perez et al*., 2011; *Zhang et al*., 2011], particularly for highly turbid and productive water bodies.

In spite of the fact that lakes represent only a small fraction of the Earth's total surface water (0.013%) [*Shiklomanov*, 1993], the variability in their absorption and scattering coefficients is likely to be far greater than that encountered in the oceans, shelf seas, and coastal waters because the close proximity of land. Surface runoff from land exerts a strong influence on the composition and concentration of dissolved and particular matter in lakes. In turn, absorption and scattering by dissolved and particulate materials affect the spectral shape and magnitude of the remote sensing reflectance ($R_{rs}(\lambda)$) measured by satellite sensors [*Morel and Prieur*, 1977; *Kirk*, 1994]. Knowledge of the variability of mass-specific inherent optical properties (SIOPs) is thus necessary for the interpretation of water-leaving reflectance signals. More formally, R_{rs} can be related to $a(\lambda)$ and $b_b(\lambda)$ via equation (1), where f is an experimental constant dependent on the light field and volume scattering function and Q is a parameter accounting for geometrical attenuation of light exiting the water column [*Gordon et al*., 1975; *Morel and Gentili*, 1991; *Dall'Olmo and Gitelson*, 2005]:

$$R_{rs}(0+,\lambda) \propto \frac{f}{Q}\frac{b_b(\lambda)}{a(\lambda)+b_b(\lambda)} \tag{1}$$

The absorption and backscattering coefficients can be further partitioned into the contributions from each optically active constituent via equations (2) and (3),

$$a(\lambda)=a_{ph}(\lambda)+a_{\mathrm{NAP}}(\lambda)+a_{\mathrm{CDOM}}(\lambda)+a_w(\lambda) \tag{2}$$

$$b_b(\lambda)=b_{b,ph}(\lambda)+b_{b,\mathrm{NAP}}(\lambda)+b_{b,w}(\lambda) \tag{3}$$

where $a_{ph}(\lambda)$, $a_{\mathrm{NAP}}(\lambda)$, $a_{\mathrm{CDOM}}(\lambda)$, and $a_w(\lambda)$ represent the absorption coefficients for phytoplankton, NAP, CDOM, and water, and $b_{b,ph}(\lambda)$, $b_{b,\mathrm{NAP}}(\lambda)$, and $b_{b,w}(\lambda)$ represent the backscattering coefficients for phytoplankton, NAP, and pure water, respectively. It is generally assumed that CDOM is nonscattering.

The relative contribution of the dissolved and particulate constituents to absorption and backscattering budgets varies significantly between different water types. Moreover, changes in size and composition of the constituents can result in marked changes in the SIOPs. For instance, the mass-specific particulate scattering coefficient [$b^*_p(555)$] was reported to vary in ocean and coastal waters based on the proportion of organic versus mineral particles, and particle water content, apparent density, and refractive index [*Babin et al*., 2003a]. The variability of SIOPs is a major source of uncertainty in the interpretation of water-leaving reflectance signals, in the retrieval of biogeochemical properties and in estimates of primary production [*Dall'Olmo and Gitelson*, 2005; *Gilerson et al*., 2010; *Tilstone et al*., 2012]. The improved parameterization of remote sensing algorithms for turbid lakes and other optically complex waters thus relies on a comprehensive knowledge of the mass-specific absorption and scattering coefficients of lake water constituents and on an understanding of the sources and magnitude of their variability across different lake types. In particular, knowledge of the absorption properties at the wavelengths of ~440, 620, and 675 nm have direct implications for the remote sensing retrievals of phytoplankton pigments, including chlorophyll-*a* (Chl-*a*) and phycocyanin (PC), in order to distinguish potentially harmful cyanobacteria blooms in lakes [*Simis et al*., 2005; *Kutser et al*., 2006; *Hunter et al*., 2010; *Mishra et al*., 2013].

The (S)IOPs of inland waters have been relatively poorly studied, but the limited research to date suggests that they exhibit significant variability. *Luis Perez et al*. [2011] found that the absorption and mass-specific absorption coefficients of particulate matter in Laguna Chascomús, Argentina show significant seasonal

variability. In Lake Taihu, both spatial and seasonal differences were found in the absorption coefficients of phytoplankton, with significantly lower $a_{ph}(440)$ and $a_{ph}(665)$ recorded in the winter [*Zhang et al*., 2010]. While no spatial differences were found in the Chl-*a*-specific absorption coefficient, $a^*_{ph}(440)$ was significantly higher in spring, and $a^*_{ph}(665)$ was highest in spring and summer in Lake Taihu [*Zhang et al*., 2010]. Seasonal variations in $a^*_{ph}(\lambda)$ in Lake Taihu have also been associated with the seasonal changes in community composition, and $a^*_{ph}(\lambda)$ increased with the succession from chlorophytes to cyanophytes [*Zhang et al*., 2012]. In contrast, in Lake Onondaga mean annual $a^*_{ph}(676)$ remained nearly uniform over a 5 year study period [*Perkins et al*., 2014]. $a^*_{ph}(440)$ was observed to decline during a particular interval where diatoms dominated, however no statistically significant or recurring trends in $a^*_{ph}(\lambda)$ were reported in this study [*Perkins et al*., 2014]. Some evidence for regional differences in SIOPs has also been reported in studies where multiple water bodies were investigated. For instance, in several eutrophic turbid inland waters in China, there were large regional differences in $a^*_{ph}(675)$ and $a^*_{NAP}(440)$, with variations in $a^*_{ph}(675)$ ranging from 0.002 to 0.285 $m^2\ mg^{-1}$ [*Shi et al*., 2013]. Another study on three productive reservoirs in South Africa found differences in $a^*_{ph}(440)$ related to trophic class and the presence of monospecific cyanobacteria blooms [*Matthews and Bernard*, 2013]. Spatial differences in optical properties within a single water body have also been reported, although chiefly with regard to IOPs rather than SIOPs. Following a wind event in western Lake Erie, spectral variations in $a(\lambda)$ and its contributing components was reported, and more modest wavelength dependencies for $b_p(\lambda)$ and $b_{bp}(\lambda)$ which were consistent with observations reported for coastal systems [*O'Donnell et al*., 2010]. Similarly, spatial heterogeneity in IOPs and apparent optical properties (AOPs) has been reported in Lake Champlain, with uncoupled variation between absorption and biogeochemical parameters [*O'Donnell et al*., 2013]. A study by *Effler et al*. [2012] demonstrated both spatial and temporal differences in the IOPs in Oneida Lake, NY, with the sum of a_{NAP}, a_{CDOM}, and a_{ph} at 440 nm ranging from 0.9 to 2.0 m^{-1} over the summer months (June–August). This study further found a high contribution from CDOM to $a(440)$, however variations in NAP and phytoplankton ultimately drove absorption dynamics. Thus, while it has been widely documented in previous studies that IOPs and AOPs are variable in both time and space along with variations in the optically active constituents (OACs), further knowledge is required to characterize the relationships between IOPs and OACs in other systems, given the wide range of biogeochemical composition in inland waters. In particular, there are few measurements of the mass-specific IOPs (SIOPs) in inland waters. Therefore, the focus of this study is to characterize the extent and cause of the spatial variability of the SIOPs within a large turbid freshwater system.

In particular, the main aims of this study are: (1) to improve our quantitative knowledge of the absorption coefficients of dissolved and particulate matter in highly productive and turbid lake systems; (2) to determine the magnitude and sources of spatial variability in the absorption coefficients of the in-water constituents across biogeochemical gradients. This study builds on previous research on the bio-optical properties of lakes by extending measurements into highly minerogenic waters with marked variability in both phytoplankton biomass and terrestrial inputs of CDOM. It is anticipated that this work will progress our understanding of the factors influencing the underwater light field and water-leaving radiative signals in lakes and inform the parameterization and selection of remote sensing algorithms for the retrieval of biogeochemical parameters in different lake optical types, including an understanding of the uncertainties and biases on the resulting products.

2. Methods

2.1. Study Site

Lake Balaton is the largest freshwater lake in central Europe by surface area (596 km^2) and one of the most intensively studied. The lake is very shallow with a mean depth of approximately 3 m and, as such, bottom sediments are frequently resuspended in the water column [*Herodek*, 1986; *Présing et al*., 2001; *Tyler et al*., 2006]. This results in high concentrations of suspended mineral particles that can readily exceed 50 $mg\ L^{-1}$ from resuspension during strong wind events. The lake is composed of four basins and an adjoining a wetland system (Kis-Balaton) to the west. The main inflow into the lake is the Zala River on the western shore, and the only outflow is a highly regulated channel at Siófok in the east. Nutrient inputs from the Zala River typically produce a pronounced trophic gradient from west to east. While the hydrobiology and hydroecology have been comprehensively studied, there is presently no published information on the optical properties of Lake Balaton.

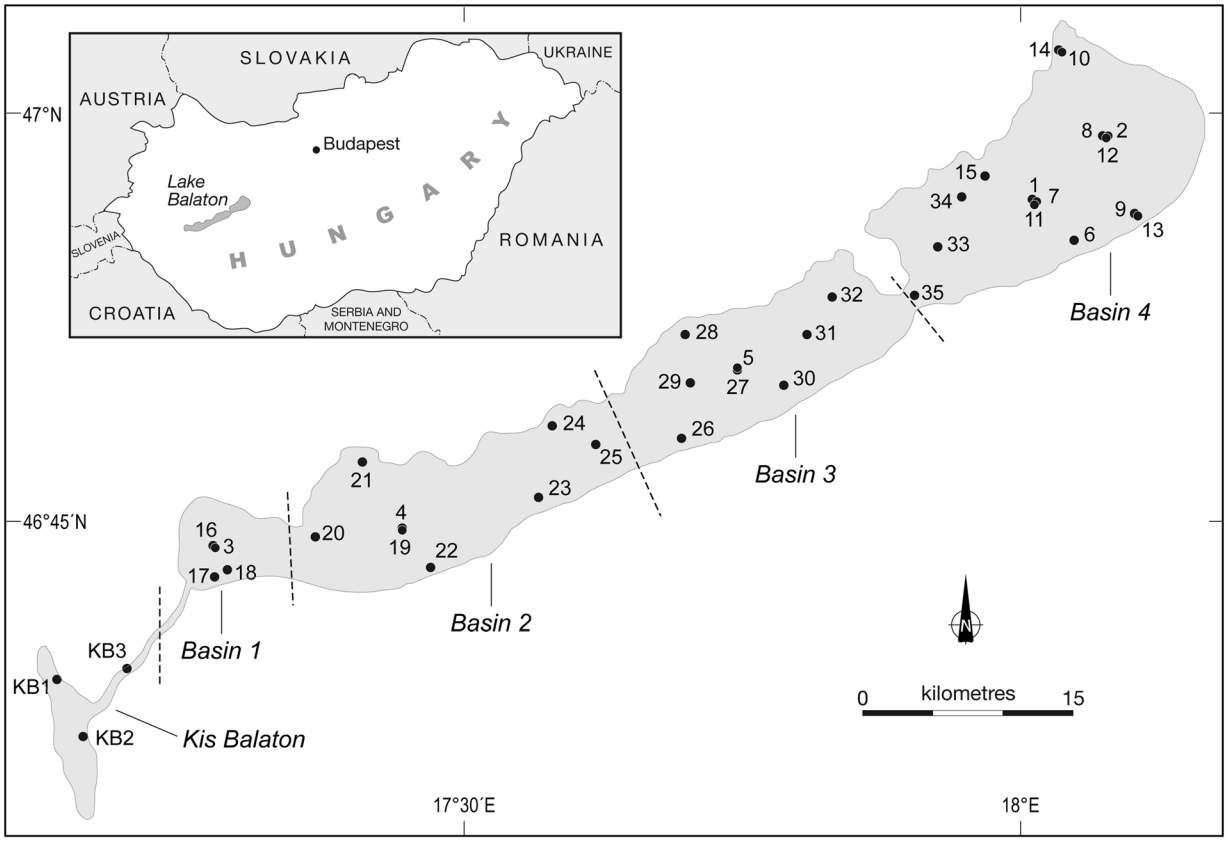

Figure 1. Map of Lake Balaton and Kis-Balaton indicating the location of the basins and 38 sampling stations.

At its worst, Lake Balaton experienced hypereutrophic conditions in its westerly basins and eutrophic conditions in eastern basins because of increased nutrient loads in the 1970s [*Herodek*, 1986]. Blooms of filamentous cyanobacteria (*Cylindrospermopsis raciborskii* (Wołoszynska) Seenayya and Subba Raju) dominated the summer plankton community in the 1980s and 1990s [*Présing et al*., 1996]. Since then, extensive waste water treatment and diversion schemes, the introduction of Kis-Balaton wetlands, closure of nearby farms in 1987, and reduction of fertilizer use have all substantially reduced nutrient loading to Lake Balaton, resulting in lower phytoplankton biomass and improved water quality [*Somlyódy et al*., 1997].

2.2. Water Sampling

Field measurements in Lake Balaton and Kis-Balaton were conducted at 38 stations over a 1 week period in August 2010 (Figure 1), with the aim of collecting data on the spatial variability in the light absorption budget over a gradient from the highly productive, high phytoplankton biomass waters in western basins and Kis-Balaton to the low chlorophyll, low CDOM waters in the eastern basins. Daily average wind speed was also measured during each sampling occasion at automatic stations in order to investigate variations in the IOPs during resuspension events (Table 1; Central-Transdanubian Water Directorate). At each station, a surface water sample was divided into subsamples for subsequent filtration or preservation. Subsamples for the determination of pigment concentrations and laboratory measurements of particulate absorption were filtered on the boat immediately after sample collection under low vacuum pressure through 25 mm GF/F filter papers (Whatman, nominal pore size 0.7 μm). Depending on the turbidity, between 20 and 70 mL of water was filtered. Filter papers were flash frozen in liquid nitrogen for $<$12 h and stored in a -80°C freezer until analysis (no more than 6 months). Further subsamples for CDOM and total suspended matter (TSM) were kept cool and in the dark on the boat and processed in the laboratory within 24 h. Finally, one subsample was collected for phytoplankton enumeration and preserved in Lugol's solution immediately after collection.

Table 1. Daily Average Wind Speed Over the Sampling Period at Basin 4 (Siófok, Lake Balaton)

Date	Average Wind Speed ($m\ s^{-1}$)[a]	Daily Maximum Wind Speed ($m\ s^{-1}$)
17 Aug	3.2	7.6
18 Aug	2.4	7.7
19 Aug	2.5	5.7
20 Aug	2.9	7.0
21 Aug	1.8	3.1
22 Aug	1.4	3.3
23 Aug	2.4	5.1
24 Aug	2.7	9.2
25 Aug	5.6	13.6
26 Aug	3.6	5.1
All dates	2.9	13.6

[a]Average of hourly wind speed measurements at Basin 4.

2.3. In Situ Optical Measurements

To measure the IOPs in situ, two optical instrument packages were deployed. The first consisted of an AC-S (WET Labs Inc.) in situ spectrophometer interfaced with a CTD (Sea-Bird Electronics) recording temperature, salinity, and pressure (depth). This package also included an ECO-BB3 (WET Labs Inc.) backscatter meter. These instruments were mounted in a black metal cage and deployed over a beam, which extended the cage approximately 1.5 m away from the boat. Simultaneously, an AC-9 (WET Labs Inc.) in situ spectrophometer was deployed with and without a 0.2 μm AcroPak filter (Pall Corporation) for separation of dissolved and particulate contributions to absorption. Because Lake Balaton is highly turbid and very well mixed, all measurements were made just below the water surface within the first optical depth. Prior to data collection, the AC-S and AC-9 were flushed and debubbled for 5 min. Five minute casts were subsequently executed at each station with the data recorded to a DH4 data logger (WET Labs Inc.).

An AC-S and AC-9 (WET Labs Inc.) were deployed to collect absorption (a) and attenuation (c) measurements. The AC-S collected hyperspectral spectra over 84 wavelengths, from 401 to 755 nm at ~4 nm resolution, while the AC-9 collected data at nine wavelengths only (412, 440, 488, 510, 532, 555, 650, 676, and 715 nm). The AC-S was only utilized in Basins 1–4, while AC-9 data were collected in Kis-Balaton as well. The AC-S or AC-9 raw data were corrected for the time lag associated with the flow rate for the instrument, then was merged with the CTD data for temperature, salinity, and pressure. Using the CTD data, the effects of temperature and salinity on pure water absorption and attenuation were removed with wavelength-dependent corrections according to *Pegau et al*. [1997]. To correct for instrument drift, a pure water calibration was subtracted from both attenuation and absorption data. The proportional scattering correction of *Zaneveld et al*. [1994] was applied to absorption data to account for inefficient collection of the scattered light within the AC-S or AC-9 reflecting tube. The proportional scattering correction is used here to be consistent with recent studies [*Leymarie et al*., 2010; *Slade et al*., 2010; *Astoreca et al*., 2012]. All AC-S and AC-9 data were also screened for any data out with two standard deviations in order to eliminate any error from bubbles or large particles.

2.4. Chlorophyll-*a*

Frozen GF/F filter papers were thawed from −80°C in the dark prior to analysis for pigments and particulate absorption. Chlorophyll-*a* (Chl-*a*) was measured in triplicate via spectrophotometry (Shimadzu UV-1601) after a hot 90% methanol extraction following *Iwamura et al*. [1970]. The hot methanol method was used here because it has been previously found to provide the most complete extraction of Chl-*a* for the phytoplankton types found in Lake Balaton (M. Présing, personal communication, 2014).

The spectrophotometric method was also validated against samples analyzed using high-performance liquid chromatography (HPLC). Pigments were extracted in acetone containing an internal standard (apo-carotenoate) after *Martinez-Vicente et al*. [2010] and separated using a reverse-phase Hypersil 3 mm C8 MOS-2 column on Thermo-separations© and Agilent© instruments with photodiode array detection [*Barlow et al*., 1997; *Llewellyn et al*., 2005]. Pigments were quantified against commercial phytoplankton pigment standards (DHI Lab Products, Denmark). The spectrophotometric Chl-*a* data showed strong agreement with Chl-*a* results determined using HPLC methods ($R^2 = 0.987$, $p < 0.001$). Results presented hereafter are based on the Chl-*a* data from spectrophotometry because the HPLC measurements were not replicated.

2.5. Phycocyanin

Phycocyanin was extracted in a solution of 15 mL 0.05 *M* phosphate buffer (pH = 6.8). The solution was then subjected to sonication over ice for 15 s (Ultrasonic Homogenizer 4710 Series with microtip and 50% duty cycle, Cole-Parmer Instrument Co., USA) as in *Horváth et al*. [2013]. The extracts were clarified by

filtration (Whatman GF/C filter) and the absorption was measured on a spectrophotometer (Shimadzu UV-1601, Shimadzu Corp., Japan). Phycocyanin concentrations were calculated using the equations of *Siegelman and Kycia* [1978]. Clear outlying values were discarded so the PC concentrations were the mean of (minimum) two replicates.

2.6. Biomass and Phytoplankton Counts

Phytoplankton species were enumerated with an inverted plankton microscope [*Utermöhl*, 1958]. The wet weight of each species was calculated from cell volumes [*Németh and Vörös*, 1986]. At least 25 cells (or filaments) of each species were measured to determine biomass and at least 400 were counted.

2.7. Total Suspended Matter

TSM was obtained by gravimetric analysis. Water (500–1500 mL) was filtered under low-vacuum pressure (<700 mbar, −50 kpa) through a preashed (furnace at 450°C) and preweighed 47 mm GF/C filter paper (Whatman). Following filtration, filter papers were dried for 24 h in a clean oven at 60°C and subsequently weighed to obtain TSM. Filters were then placed in a furnace at 450°C overnight and subsequently weighed to obtain particulate inorganic matter (PIM). Particulate organic matter (POM) was calculated as the difference between TSM and PIM.

2.8. Colored Dissolved Organic Matter Absorption

Water samples were filtered into clean glassware through 0.2 μm nucleopore membrane filters (Whatman) and measured according to *Tilstone et al*. [2002] within 24 h of collection. Absorption of the filtrate was determined on a spectrophotometer (Shimadzu UV-1601) with a 5 cm quartz glass cuvette over the range of 350–800 nm, using MilliQ water as a reference. The absorption coefficient of CDOM (a_{CDOM}) was calculated using the following equation:

$$a_{CDOM}(\lambda) = 2.303 D(\lambda)/r \quad (4)$$

where $D(\lambda)$ is the measured absorption at a given wavelength and r is the cuvette path length in meters. A baseline correction was applied by subtracting the mean value of $a_{CDOM}(\lambda)$ in 5 nm interval around 685 nm [*Babin et al*., 2003b]. This wavelength was used because there is negligible a_{CDOM} at 685 nm and the effects of temperature and salinity on water absorption are small [*Pegau et al*., 1997]. The spectral slope of the CDOM absorption curve (S_{CDOM}) was calculated over the wavelength range of 400–500 nm using an exponential function fitted by nonlinear regression [*Twardowski et al*., 2004; *Perkins et al*., 2009].

2.9. Laboratory Measurement of Particulate Absorption

The absorbance of the material on the filter was measured from 350 to 750 nm according to the "transmittance-reflectance" method of *Tassan and Ferrari* [1998] using a dual beam spectrophotometer (Lambda 2, PerkinElmer Inc.) retro-fitted with a spectralon coated integrating sphere. Absorption was measured before and after bleaching with a 1% solution of NaClO to obtain total particulate absorption ($a_p^{spec}(\lambda)$) and absorption by nonalgal particles ($a_{NAP}(\lambda)$), respectively. The path length amplification correction of *Tassan and Ferrari* [1998] was applied, and absorption by phytoplankton ($a_{ph}(\lambda)$) was calculated as the difference between $a_p^{spec}(\lambda)$ and $a_{NAP}(\lambda)$. Chlorophyll-specific absorption coefficients ($a^*_{ph}(\lambda)$) were obtained by dividing $a_{ph}(\lambda)$ by the respective Chl-*a* concentration. An exponential function was fitted by nonlinear regression to the $a_{NAP}(\lambda)$ spectra, and the spectral slope of $a_{NAP}(\lambda)$ (S_{NAP}) was obtained. Wavelengths 350–750 nm were used in fitting the exponential function, disregarding the ranges 400–480 and 620–710 nm to avoid any residual pigment absorption, as in *Babin et al*. [2003b]. The data from three stations (26, 27, and 30) were discarded for the purposes of S_{NAP} calculation due to spectral artifacts and extremely low values of $a_{NAP}(440)$.

3. Results

3.1. Comparison of In Situ and Laboratory-Measured Absorption

Bulk absorption coefficients ($a(\lambda)$, m^{-1}) measured in situ were compared with summed laboratory measurements of particulate and CDOM absorption ($a(\lambda) = a_p(\lambda) + a_{CDOM}(\lambda)$). Linear regressions of laboratory and in situ total absorption measurements at three wavelengths (440, 555, and 676 nm) are shown in Figure 2. There was some agreement between in situ and laboratory measurements, with roughly the same

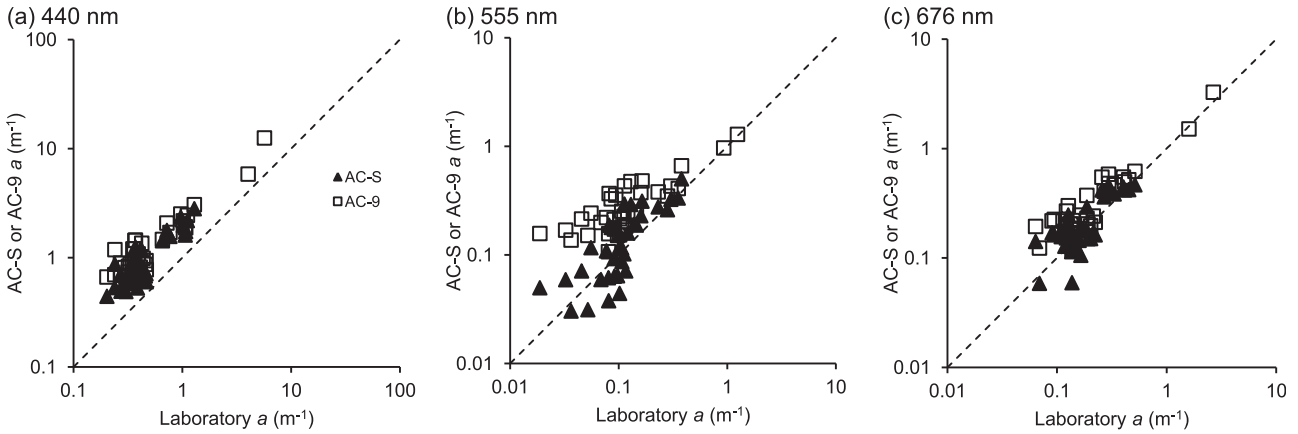

Figure 2. Comparison of total nonwater absorption ($a(\lambda) = a_{ph}(\lambda) + a_{NAP}(\lambda) + a_{CDOM}(\lambda)$) from in situ (AC-S or AC-9) or laboratory methods at (a) 440, (b) 555, and (c) 676 nm. Axes are on logarithmic scale and dashed line represents the 1:1 line.

distribution but some differences in absolute values. In situ measurements generally correlated well with laboratory measurements, with R^2 values of 0.743–0.843 ($p < 0.001$) for the AC-S and 0.871–0.967 ($p < 0.001$) for the AC-9. However, there was a particular lack of sensitivity in the AC-9 and, to a lesser extent, the AC-S data to variations in absorption at 555 nm. Additionally, in situ measurements overestimated laboratory total absorption at these wavelengths by a factor of 1.1–2.1 (AC-S) and 1.5–2.5 (AC-9), with improved agreement in the red portion of the spectrum (676 nm) (Figure 2). In contrast, a previous study by *Leymarie et al*. [2010] found measured $a(\lambda) + a_w(\lambda)$ (total nonwater and water absorption) to be underestimated when using the proportional scattering correction, with the errors highest in the red portion of the spectrum. In the present study, it is expected that the overestimate of absorption is due to the scattering errors in the AC-9 and AC-S measurements which were not resolved by the proportional scattering correction [*Mckee et al*., 2008]. Scattering increases at shorter wavelengths, thus a smaller difference (i.e., better agreement) would exist between the in situ and laboratory absorption measurements at longer wavelengths. Furthermore, there was a marked discrepancy between the two data sets of in situ absorption coefficients (at 440 nm, absolute error = 0.041–0.31 m^{-1}). In general, the lab data more accurately reflected the spatial variability in absorption and had greater sensitivity, particularly in waters with low absorption. Thus, for the purpose of this study, laboratory measured absorption and specific absorption coefficients will be considered only, and in situ results are solely presented in the methods for comparison.

3.2. Variability in Optically Active Constituents

The Chl-*a* and TSM data collected during the sampling campaign are shown in Figure 3 in relation to the annual cycle for these parameters. In all four basins, Chl-*a* concentrations peaked in early August immediately prior to the sampling campaign due to the development of a cyanobacterial bloom over much of the lake and remained high during the sampling campaign in three of the four basins. TSM concentrations were more variable over the year, with a marked peak in early summer in all basins and a winter peak in Basin 1 due to wind-driven resuspension. The sampling campaign was undertaken during a period with TSM concentrations mostly slightly lower than the annual mean (22 ± 21 mg L^{-1}) but these were not atypical for Lake Balaton.

The stations sampled in Lake Balaton and Kis-Balaton during summer 2010 demonstrated significant variability in the concentration of optically active constituents (Table 2). Mean Chl-*a* concentrations ranged from ~160 mg m^{-3} in Kis-Balaton to ~10 mg m^{-3} in Basin 4, and phytoplankton biomass ranged from ~70,000 to ~2800 mg m^{-3}, over the trophic gradient from west to east across the system. TSM ranged from ~40 mg L^{-1} in Kis-Balaton to 13 mg L^{-1} in Basin 4, with POM comprising the majority of TSM in Kis-Balaton (67%) and PIM comprising the majority of TSM in Basins 1–4. The greatest contribution of PIM to TSM (81%) was observed in Basin 3. Chl-*a* was strongly linearly correlated with POM ($R^2 = 0.97$, $p < 0.001$, $n = 38$) with mean Chl-*a*:POM = 0.00395 ± 0.00110. Total phytoplankton biomass was also linearly correlated with POM ($R^2 = 0.88$, $p < 0.001$, $n = 38$) with mean total biomass:POM = 0.998 ± 0.583. The mean PC:POM ratio for all basins is 0.00321 ± 0.00145 ($R^2 = 0.75$, $p < 0.001$, $n = 38$), although this linear

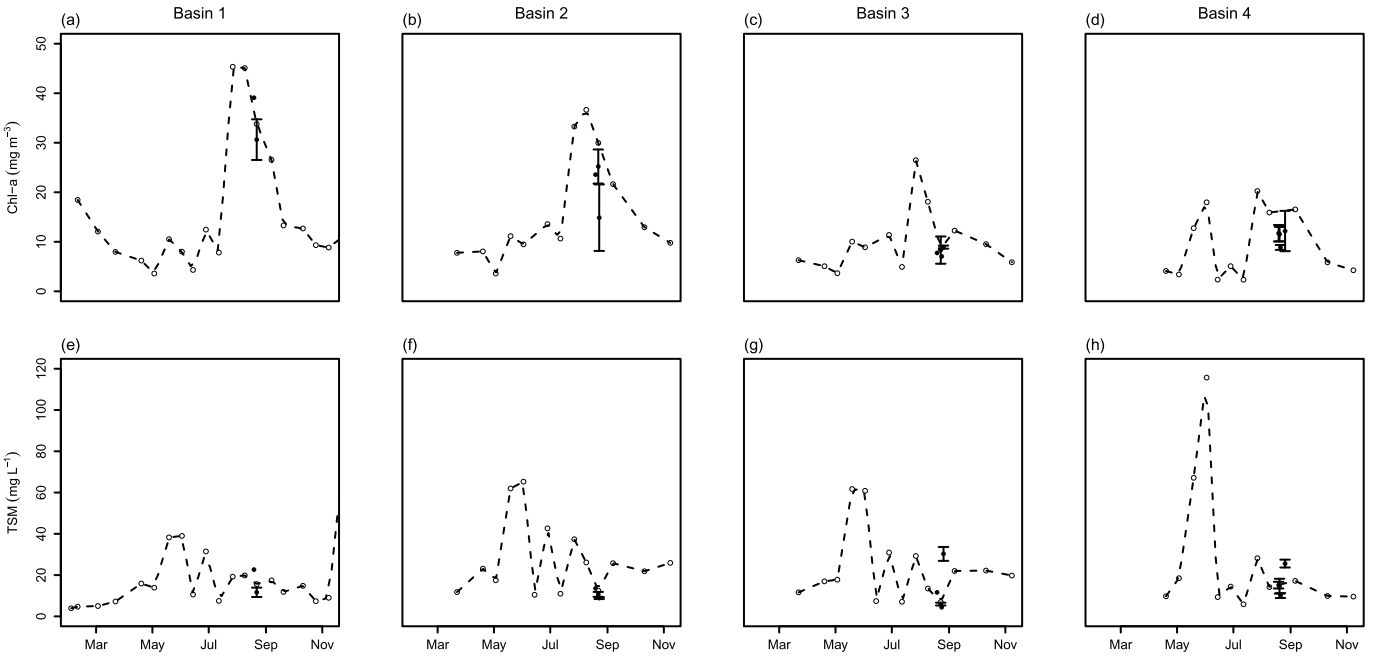

Figure 3. (a–d) Annual variation in chlorophyll-*a* (Chl-*a*) concentrations and (e–h) total suspended matter (TSM) concentrations for 2010 in Lake Balaton Basins 1–4. Solid dots are mean daily values measured during the August 2010 campaign, with error bars indicating standard deviation. Annual data provided by the routine monitoring at a single station in each basin by the Balaton Limnological Institute.

relationship had more dispersion than that for Chl-*a* or total biomass with POM. Stations in the east of Basin 3 and west of Basin 4 had markedly higher concentrations of TSM because wind-driven resuspension of bottom material was more prevalent in these basins during sampling than elsewhere. Chl-*a*, PC and ratios of POM and PIM at each station are shown in Figure 4, while the gradients in Chl-*a* and PC concentrations over distance from the Zala River are presented in Figure 5.

Cyanobacteria biomass was found to correlate strongly with measured PC concentrations ($R^2 = 0.97$, $p < 0.001$, $n = 38$), and total biomass showed a strong linear relationship with Chl-*a* ($R^2 = 0.96$, $p < 0.001$, $n = 38$). PC concentrations were highest in Kis-Balaton (156 mg m^{-3}) with decreasing concentrations from Basins 1 to 3 (22–6 mg m^{-3}) and a slight increase in Basin 4 (10 mg m^{-3}), which corresponds to the abundance of nitrogen fixing cyanobacteria (Figure 4). In almost all stations, cyanobacteria comprised the majority of the phytoplankton (up

Table 2. Mean Biogeochemical Parameters (Standard Deviation) for Each Basin and Kis-Balaton[a]

	Kis-Balaton ($n = 3$)	Basin 1 ($n = 4$)	Basin 2 ($n = 8$)	Basin 3 ($n = 8$)	Basin 4 ($n = 15$)	Lake Mean[b] ($n = 35$)	Units
Chl-*a*	166.51 (83.15)	32.74^{c,d,e} (5.40)	21.12^{d,e,f} (6.71)	8.24^{c,f} (1.91)	10.80^{c,f} (2.30)	15.08 (8.90)	mg m^{-3}
PC	156.27 (176.68)	22.33^{d,e} (7.41)	15.62^{d} (4.56)	6.19^{c,f} (2.05)	9.95^{f} (2.67)	11.80 (6.19)	mg m^{-3}
TSM	40.98 (13.28)	14.41^{g} (5.82)	10.36^{g} (1.78)	12.55^{g} (11.23)	15.37^{g} (6.11)	13.47 (7.01)	mg L^{-1}
POM	27.53 (8.63)	6.09^{d,e} (1.23)	4.71^{d,e} (1.41)	2.41^{c,f} (0.53)	3.41^{c,f} (0.49)	3.78 (1.43)	mg L^{-1}
PIM	13.44 (11.54)	8.32^{g} (4.79)	5.65^{g} (1.63)	10.14^{g} (10.96)	11.97^{g} (6.04)	9.69 (6.98)	mg L^{-1}
Total Biomass	70839 (53637)	7062^{c,d,e} (1780)	3916^{d,f} (1376)	1854^{c,f} (603)	2851^{f} (821)	3348 (1832)	mg m^{-3}
Cyano Biomass	55876 (58954)	5756^{c,d,e} (1810)	3456^{d,f} (1163)	1232^{c,f} (759)	2134^{f} (671)	2644 (1658)	mg m^{-3}
Cyano Biomass	57 (50)	81^{g} (8)	88^{g} (6)	64^{g} (27)	74^{g} (17)	76 (19)	%

[a]Chl-*a*, chlorophyll-*a* measured by spectrophotometry; PC, phycocyanin; TSM, total suspended matter; POM, particulate organic matter; PIM, particulate inorganic matter; Total Biomass, all phytoplankton biomass; Cyano Biomass, cyanobacteria biomass only. Numerical superscripts designate statistically significant differences between the respective parameter in Basins 1–4 using Tukey's Honest Significant Difference method ($p < 0.01$, adjusted for multiple comparisons)

[b]Significantly different to Basin 1.

[c]Significantly different to Basin 2.

[d]Significantly different to Basin 3.

[e]Significantly different to Basin 4.

[f]Lake Mean includes the 35 stations in the main basins only (not including Kis-Balaton).

[g]Not significantly different from any basin.

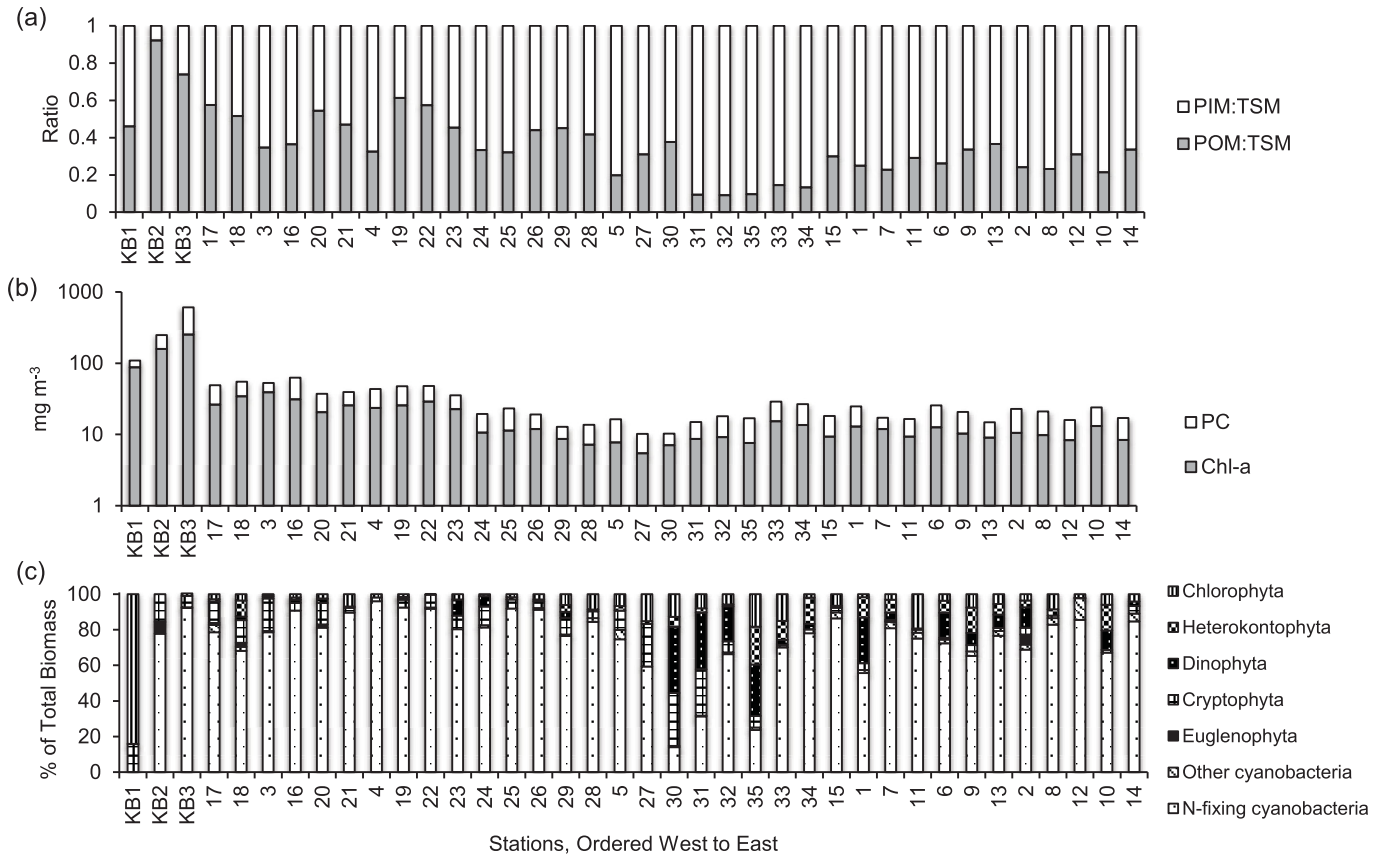

Figure 4. Barplots of the ratio of (a) particulate inorganic matter (PIM:TSM) and particulate organic matter (POM:TSM), (b) chlorophyll-*a* (Chl-*a*) and phycocyanin (PC) concentrations, and (c) phytoplankton community composition as percentage of total biomass at all stations in order from west to east.

to 96%) with the most abundant species being the nitrogen-fixing cyanobacterium *Cylindrospermopsis raciborskii*, which typically comprised over 50% of the cyanobacterial biomass in the lake. Phytoplankton composition at each station is shown in Figure 4c, indicating the dominance of nitrogen-fixing cyanobacteria, with an increasing presence of cryptophytes, chlorophytes, dinophytes, and heterokontophytes in Basins 3 and 4.

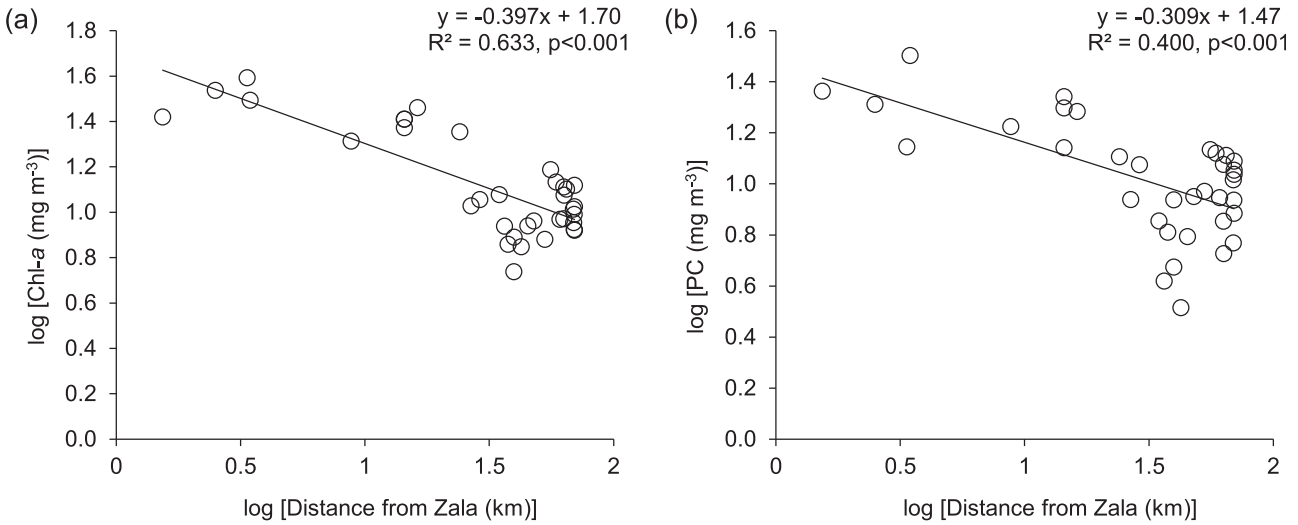

Figure 5. Plots of (a) chlorophyll-*a* (log[Chl-*a* (mg m^{-3})]) and (b) phycocyanin (log[PC (mg m^{-3})]) as a function of distance from the Zala River during the Lake Balaton sampling campaign.

Unusual stations to note include KB1, 30, 31, and 35. KB1 is nearest to the inflow from the Zala River and this area typically has lower biomass than the rest of Kis-Balaton, and generally has lower cyanobacteria biomass as well. In 2010, the inflow was high and this prevented the development of cyanobacterial blooms (M. Présing, personal communication, 2014). Stations 30, 31, and 35 had low percentages of N-fixing cyanobacteria and larger communities of cryptophytes and dinophytes present, although total cell biomass was relatively low (<2100 mg m^{-3}). These three stations were sampled on 24 and 26 August 2010, when high wind speeds caused increased turbulent mixing (Table 1), potentially encouraging the dominance of larger phytoplankton cells (e.g., dinoflagellates) at the surface.

Chl-*a*, CDOM, and TSM were plotted against each other in order to investigate the relationships between these OACs (Figure 6). A weak but significant linear relationship was found between log(TSM) and log(Chl-*a*) ($R^2 = 0.306$, $p < 0.001$, $n = 38$; Figure 6a), similar to that reported for Lake Taihu [*Zhang et al*., 2010] and European coastal waters [*Babin et al*., 2003b]. However, the increased scatter around this relationship in Lake Balaton is likely attributed to the large proportion of minerals in the suspended matter. Log($a_{CDOM}(440)$) and log(Chl-*a*) also covaried linearly (Figure 6b; $R^2 = 0.714$, $p < 0.001$, $n = 38$), a relationship that has been reported in a range of coastal waters [*Babin et al*., 2003b]. In Lake Balaton, this is likely due to the fact that both CDOM and Chl-*a* decrease with increasing distance from the Zala River. However, this relationship broke down in Kis-Balaton and Basin 1, which are closest to the river inflow. No significant linear relationship was reported between log($a_{CDOM}(440)$) and log(TSM) ($R^2 = 0.132$, $p = 0.025$, $n = 38$; Figure 6c). Again, in Lake Balaton, much of the TSM was comprised of PIM due to resuspension, thus a strong relationship with CDOM was not expected.

As the campaign was conducted over several days, any effect of sampling date on the measured concentrations was assessed using a generalized linear model, and the only significant relationship was observed for PIM ($p < 0.001$). This was likely due to differences in the wind-driven resuspension of mineral particles from the lake bottom. Thus, most of the variability observed in the biogeochemical constituents can be assumed to be due to local differences in fluvial input, biological productivity and in-lake processing of particulate and dissolved material.

3.3. Variability in the Inherent Optical Properties

In general, the IOPs were variable across the system, with the most distinctly different properties exhibited in the westernmost portion, Kis-Balaton (Table 4). As with biogeochemical parameters, the measured (S)IOPs were tested for the effect of sampling date using a generalized linear model. $a_p(440)$ was the only parameter with a significant relationship with sampling date ($p < 0.001$). Figure 7 illustrates the gradients of $a_{ph}(440)$, $a_{NAP}(440)$, and $a_{CDOM}(440)$ across the lake over increasing distance from the Zala River. Tables 3–5 summarize the bulk and specific IOPs and statistics for the four basins and Kis-Balaton, and Table 6 provides a summary of the optical properties of other large lakes from selected previous studies for comparison.

The relative contributions of optically active substances to total absorption for the 38 stations sampled on Lake Balaton are shown in Figure 8 for selected wavelengths. At all wavelengths (440, 555, 620, and 675 nm), $a_{NAP}(\lambda)$ was the smallest contributor, consistently making up less than 35% of the total absorption. At 440 nm, a_{CDOM} comprised between 33 and 76% and a_{ph} between 23 and 62% of absorption, while at 555 nm there was a wider range of composition with no clear trend by basin. Absorption at 620 nm included a higher percentage of absorption by phytoplankton (39–95%), although up to 48% and 32% were attributed to a_{CDOM} and a_{NAP}, respectively. At 675 nm over 70% of absorption was due to a_{ph} at all sites, with less than 10% due to a_{CDOM} and up to 23% due to a_{NAP}, although it was noted that CDOM and NAP had a greater contribution at 620 nm as compared to 675 nm. Thus, a_{NAP} and a_{CDOM} can contribute markedly to absorption at the wavelengths where PC and Chl-*a* absorb strongly (620 and 675 nm).

3.3.1. CDOM Absorption

CDOM absorption at 440 nm in Lake Balaton ranged from 0.093 to 2.93 m^{-1}. There was a gradient of $a_{CDOM}(\lambda)$ across the lake (Figure 9), with $a_{CDOM}(440)$ highest in the west (Kis-Balaton, 2.82 m^{-1}) where the Zala River enters and lowest in the east (Basin 4, 0.18 m^{-1}). Additionally, the difference in $a_{CDOM}(440)$ was statistically significant between the four basins (Table 5). The mean value for the spectral slope of CDOM (S_{CDOM}) was 0.018 nm^{-1} in Kis-Balaton and 0.020 nm^{-1} in the Lake Balaton.

S_{CDOM} was found to decrease exponentially with increasing $a_{CDOM}(440)$ ($p < 0.001$, $n = 38$; Figure 10). However, this relationship is driven by the larger range of S_{CDOM} values in Basin 4, and the mean S_{CDOM}

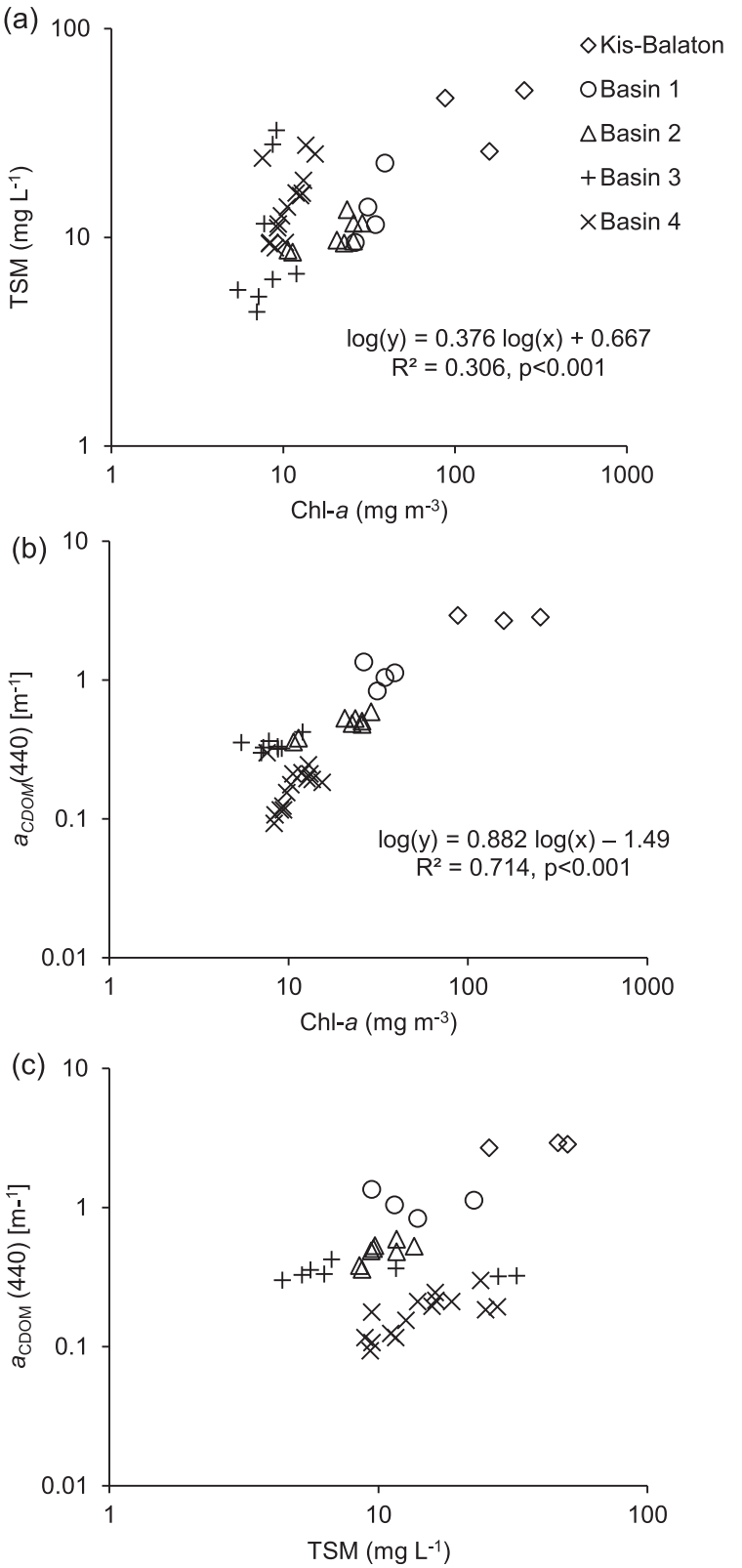

Figure 6. (a) Total suspended matter (TSM) as a function of chlorophyll-*a* (Chl-*a*) and CDOM absorption at 440 nm ($a_{CDOM}(440)$) as a function of (b) Chl-*a* and (c) TSM. Equations represent significant linear regressions on log-transformed data.

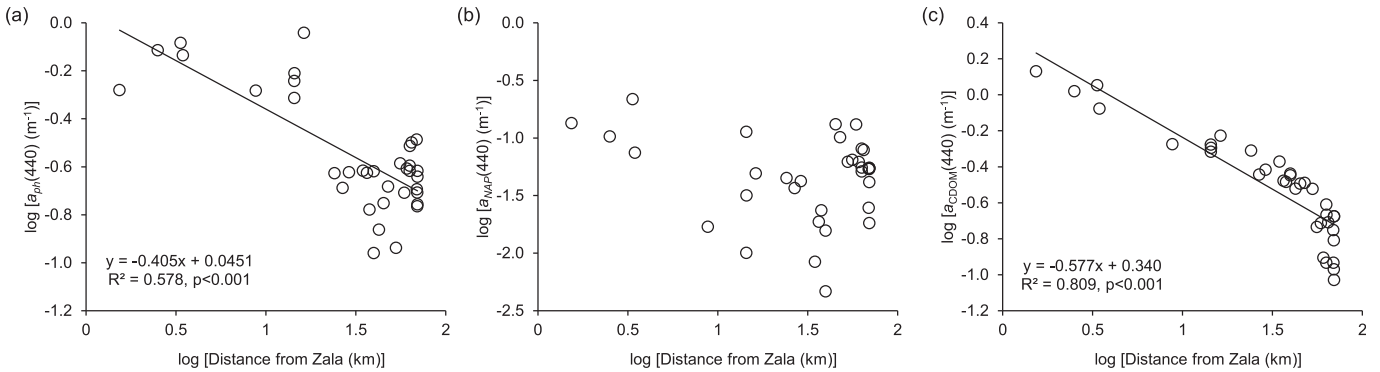

Figure 7. Plots of (a) log(a_{ph}(440) [m^{-1}]), (b) log(a_{NAP}(440) [m^{-1}]), and (c) log(a_{CDOM}(440) [m^{-1}]) as a function of distance from the Zala River during the Lake Balaton sampling campaign.

excluding Basin 4 varied over a much narrower range (0.0183 ± 0.000822). There was no significant difference in S_{CDOM} values across the four basins (ANOVA $p > 0.01$). Stations in Basin 4 had the greatest range in S_{CDOM} (0.015–0.041 nm^{-1}), whereas the S_{CDOM} values in the western basins and Kis-Balaton had much less variation (Table 5). This is likely due to the large influence of the Zala River on CDOM concentrations in the west of Lake Balaton, while complex interactions between localized fluvial inputs and increased contributions from authochthonous sources (phytoplankton decomposition) may play a larger role in the more variable CDOM concentrations observed in the east of the lake.

3.3.2. Phytoplankton Absorption

Particulate absorption at 440 (a_p(440)) was generally dominated by phytoplankton, with a_{ph}(440) contributing up to 90% of the total particulate absorption (Basin 2). Phytoplankton absorption coefficients at 620 and 675 nm exhibited a decreasing gradient from west to east, with the lowest a_{ph} at both wavelengths in Basin 3. Mean a_{ph}(675) ranged from 0.078 m^{-1} (Basin 3) to 1.55 m^{-1} (Kis-Balaton), and a_{ph}(620) ranged from 0.038 m^{-1} (Basin 3) to 0.85 m^{-1} (Kis-Balaton) (Table 5).

Chl-*a* concentration showed a strong relationship with a_{ph}(440) ($R^2 = 0.93$, $p < 0.001$, $n = 38$; Figure 11a), although a greater amount of scatter was noted around 10 mg m^{-3} Chl-*a* with a slightly steeper slope than that found for oceans [*Bricaud et al.*, 1995]. Chl-*a* was also related to a_{ph}(675), with a coefficient of determination of 0.95 for a fit by least squares ($p < 0.001$, $n = 38$; Figure 11b). Similarly, phycocyanin concentrations were positively correlated with phytoplankton absorption at 620 nm, but phycocyanin itself only explained 81% of the variability in a_{ph}(620) (Figure 11c). However, when Chl-*a* and PC were summed, 93% of the variability in a_{ph}(620) was explained, which reflects the contribution of Chl-*a* to phytoplankton absorption at 620 nm (Figure 11d).

Table 3. Absorption Coefficients, Main Basins[a]

IOP	Min	Median	Max	Mean	SD	Units
a_{CDOM}(440)	0.093	0.32	1.35	0.39	0.30	m^{-1}
S_{CDOM}(400–500)	0.015	0.018	0.041	0.020	0.0057	nm^{-1}
a_p(440)	0.11	0.31	1.04	0.39	0.24	m^{-1}
a_p(675)	0.050	0.12	0.49	0.17	0.11	m^{-1}
a_{NAP}(440)	0.00	0.054	0.22	0.059	0.046	m^{-1}
S_{NAP}[b]	0.011	0.013	0.025	0.015	0.0039	nm^{-1}
a_{ph}(350)	0.057	0.15	0.46	0.18	0.094	m^{-1}
a_{ph}(440)	0.11	0.24	0.91	0.33	0.22	m^{-1}
a_{ph}(620)	0.020	0.049	0.24	0.073	0.053	m^{-1}
a_{ph}(675)	0.048	0.11	0.45	0.16	0.11	m^{-1}
a^*_{ph}(350)	0.0036	0.012	0.029	0.013	0.0061	$m^2\ mg^{-1}$
a^*_{ph}(440)	0.010	0.022	0.032	0.022	0.0046	$m^2\ mg^{-1}$
a^*_{ph}(620)	0.0029	0.0045	0.0083	0.0047	0.0011	$m^2\ mg^{-1}$
a^*_{ph}(675)	0.0055	0.0095	0.010	0.010	0.0020	$m^2\ mg^{-1}$

[a]Data include four basins of Lake Balaton only ($n = 35$).
[b]Results for S_{NAP} disregards stations 26, 27, and 30 ($n = 32$).

Table 4. Absorption Coefficients, Kis-Balaton[a]

IOP	Min	Median	Max	Mean	SD	Units
$a_{CDOM}(440)$	2.69	2.85	2.93	2.82	0.12	m^{-1}
$S_{CDOM}(400–500)$	0.017	0.018	0.018	0.018	0.00058	nm^{-1}
$a_p(440)$	1.89	3.32	4.94	3.38	1.52	m^{-1}
$a_{NAP}(440)$	0.30	0.49	0.54	0.44	0.13	m^{-1}
S_{NAP}	0.011	0.012	0.013	0.012	0.0011	nm^{-1}
$a_{ph}(350)$	1.58	1.79	2.02	1.80	0.22	m^{-1}
$a_{ph}(440)$	1.40	3.02	4.39	2.94	1.50	m^{-1}
$a_{ph}(620)$	0.34	0.77	1.44	0.85	0.55	m^{-1}
$a_{ph}(675)$	0.60	1.51	2.52	1.55	0.96	m^{-1}
$a^*_{ph}(350)$	0.0080	0.011	0.018	0.012	0.0051	$m^2\ mg^{-1}$
$a^*_{ph}(440)$	0.016	0.017	0.019	0.017	0.0015	$m^2\ mg^{-1}$
$a^*_{ph}(620)$	0.0039	0.0049	0.0057	0.0048	0.00089	$m^2\ mg^{-1}$
$a^*_{ph}(675)$	0.0069	0.0095	0.0099	0.0088	0.0017	$m^2\ mg^{-1}$

[a]Data include Kis-Balaton stations only ($n = 3$).

Phytoplankton absorption coefficients were also strongly related to phytoplankton biomass. Using nonlinear regression by least squares fit, 88% of the variability in $a_{ph}(675)$ was explained by total phytoplankton biomass, while 73% of that in $a_{ph}(620)$ was explained by cyanobacteria biomass. However, using a sum of cyanobacteria and cryptophyte biomass, a higher percentage of variability in $a_{ph}(620)$ was explained (84%). Higher $a_{ph}(675)$ and $a_{ph}(620)$ values corresponded with increased total phytoplankton and cyanobacteria biomass, respectively (Figure 12).

Mass-specific phytoplankton absorption spectra are shown for the four basins and Kis-Balaton in Figure 13. All stations show the distinctive Chl-*a* absorption maxima peaks at ~440 nm and 675 nm, and all stations (except for KB1) demonstrate a smaller absorption peak at ~620 nm due to the presence of phycocyanin. Stations in Basins 3 and 4 also had distinct peaks in the UV portion of the spectrum at approximately 360 nm, which were not visible in the spectra for Kis-Balaton and Basins 1 and 2.

The mean Chl-*a*-specific absorption coefficient at 440 nm ($a^*_{ph}(440)$) was 0.022 $m^2\ mg^{-1}$ in Lake Balaton and 0.017 $m^2\ mg^{-1}$ in Kis-Balaton (Tables 3 and 4). There was greater variation in mean $a^*_{ph}(440)$ across the basins and Kis-Balaton than observed for mean a^*_{ph} (675), ranging from 0.017 to 0.023 $m^2\ mg^{-1}$ (Tables 4 and 5). The mean $a^*_{ph}(675)$ for the four lake basins was 0.010 $m^2\ mg^{-1}$ (Table 3) and was slightly lower in Kis-Balaton (0.0088 $m^2\ mg^{-1}$; Table 4). Mean values for $a^*_{ph}(675)$ showed little variation across the basins and Kis-Balaton, with a narrow range of 0.0088–0.011 $m^2\ mg^{-1}$ (Tables 4 and 5).

Table 5. Mean Absorption Coefficients (Standard Deviation) by Basin[a]

IOP	Basin 1 ($n = 4$)		Basin 2 ($n = 8$)		Basin 3 ($n = 8$)		Basin 4 ($n = 15$)		Units
$a_{CDOM}(440)$	$1.09^{b,d}$	(0.21)	$0.48^{d,e}$	(0.077)	$0.34^{d,e}$	(0.038)	$0.18^{b,e}$	(0.058)	m^{-1}
S_{CDOM} (400–500)	0.018^{f}	(0.00058)	0.018^{f}	(0.00071)	0.019^{f}	(0.00076)	0.023^{f}	(0.0079)	nm^{-1}
$a_p(440)$	$0.85^{b,d}$	(0.16)	$0.52^{c,e}$	(0.24)	$0.23^{b,e}$	(0.074)	$0.29^{b,e}$	(0.064)	m^{-1}
$a_{NAP}(440)$	$0.13^{b,d}$	(0.062)	0.043^{e}	(0.031)	0.037^{e}	(0.050)	0.059^{e}	(0.026)	m^{-1}
S_{NAP}	0.013^{f}	(0.00090)	0.017^{f}	(0.0048)	0.017^{f}	(0.0048)	0.014^{f}	(0.0029)	nm^{-1}
$a_{ph}(350)$	0.29^{f}	(0.048)	0.21^{f}	(0.13)	0.14^{f}	(0.049)	0.15^{f}	(0.073)	m^{-1}
$a_{ph}(440)$	$0.71^{c,d}$	(0.13)	$0.47^{c,d}$	(0.24)	$0.19^{b,e}$	(0.050)	$0.23^{b,e}$	(0.058)	m^{-1}
$a_{ph}(620)$	$0.17^{c,d}$	(0.019)	$0.11^{c,d}$	(0.062)	$0.038^{b,e}$	(0.012)	$0.049^{b,e}$	(0.015)	m^{-1}
$a_{ph}(675)$	$0.36^{b,d}$	(0.078)	$0.22^{c,e}$	(0.11)	$0.078^{b,e}$	(0.020)	$0.11^{b,e}$	(0.026)	m^{-1}
$a^*_{ph}(350)$	0.0092^{f}	(0.0020)	0.0096^{f}	(0.0039)	0.016^{f}	(0.0051)	0.014^{f}	(0.0067)	$m^2\ mg^{-1}$
$a^*_{ph}(440)$	0.022^{f}	(0.0060)	0.022^{f}	(0.0041)	0.023^{f}	(0.0048)	0.022^{f}	(0.0015)	$m^2\ mg^{-1}$
$a^*_{ph}(620)$	0.0052^{f}	(0.00047)	0.0048^{f}	(0.0016)	0.0046^{f}	(0.00083)	0.0045^{f}	(0.0012)	$m^2\ mg^{-1}$
$a^*_{ph}(675)$	0.011^{f}	(0.00067)	0.010^{f}	(0.0028)	0.0094^{f}	(0.0011)	0.010^{f}	(0.0021)	$m^2\ mg^{-1}$

[a]Numerical superscripts designate statistically significant differences between the respective parameter in Basins 1–4 using Tukey's Honest Significant Difference method ($p < 0.01$, adjusted for multiple comparisons).
[b]Significantly different to Basin 1.
[c]Significantly different to Basin 2.
[d]Significantly different to Basin 3.
[e]Significantly different to Basin 4.
[f]No significant differences between basins.

Table 6. IOP and SIOPs From Selected Previous Studies for Comparison

(S)IOP	Min	Max	Mean	SD	Units	Location	Source
$a_{CDOM}(440)$	0.33	45.89	7.99	7.93	m^{-1}	Chagan Lake	*Wang et al.* [2011]
$a_{CDOM}(440)$	0.11	2.00			m^{-1}	Western Lake Erie	*O'Donnell et al.* [2010]
$a_{CDOM}(440)$	0.073	0.234	0.145	0.049	m^{-1}	Lake Superior	*Effler et al.* [2010]
	0.105	1.607	0.186	0.439			
$a_{CDOM}(440)$	0.27–0.46	1.52– 2.36	0.71–0.91	0.20–0.35	m^{-1}	Lake Taihu	*Zhang et al.* [2010]
$a_{CDOM}(440)$	0.08	0.75	0.23		m^{-1}	Lake Erie	*Binding et al.* [2008]
$a_{CDOM}(440)$	0.27–0.38	1.52–2.36	0.71–0.98	0.26–0.22	m^{-1}	Lake Taihu	*Zhang et al.* [2007]
$a_{CDOM}(442)$	0.43	14.5	2.65		m^{-1}	15 boreal lakes	*Ylöstalo et al.* [2014]
S_{CDOM} (400–500)			0.0165		nm^{-1}	Lake Erie	*O'Donnell et al.* [2010]
S_{CDOM} (400–500)	0.0090–0.0111	0.0139–0.0169	0.0107–0.0134	0.0016–0.002	nm^{-1}	Lake Superior	*Effler et al.* [2010]
$S_{CDOM}(350–500)$	0.011	0.025	0.0176	0.0020	nm^{-1}	European coastal waters	*Babin et al.* [2003b]
$S_{CDOM}(400–500)$	0.0178	0.0190	0.0186		nm^{-1}	Oneida Lake	*Effler et al.* [2012]
$S_{CDOM}(350–700)$	0.0155	0.020	0.0182		nm^{-1}	15 boreal lakes	*Ylöstalo et al.* [2014]
$S_{NAP}(482–618,712–750)$	0.0113	0.0145	0.0128		nm^{-1}	Oneida Lake	*Effler et al.* [2012]
$S_{NAP}(380–400,480–620,710–730)$	0.0089	0.0178	0.0123	0.0013	nm^{-1}	European coastal waters	*Babin et al.* [2003b]
$S_{NAP}(482–618,712–730)$			0.013		nm^{-1}	Western Lake Erie	*Peng and Effler* [2013]
$a^*_{ph}(440)$	0.005	0.084	0.018–0.056	0.007–0.021	$m^2\ mg^{-1}$	Three small reservoirs	*Matthews and Bernard* [2013]
$a^*_{ph}(440)$			0.026	0.008	$m^2\ mg^{-1}$	Lake Kasumigaura	*Yoshimura et al.* [2012]
$a^*_{ph}(440)$	0.013	0.505	0.086		$m^2\ mg^{-1}$	Lake Erie	*Binding et al.* [2008]
$a^*_{ph}(440)$			0.033		$m^2\ mg^{-1}$	Laurentian Great Lakes	*Perkins et al.* [2013]
$a^*_{ph}(440)$			0.035		$m^2\ mg^{-1}$	Onondaga Lake	*Perkins et al.* [2014]
$a^*_{ph}(440)$			0.048–0.083	0.012–0.021	$m^2\ mg^{-1}$	Lake Taihu	*Huang et al.* [2015]
$a^*_{ph}(443)$[a]	~0.008	~0.095			$m^2\ mg^{-1}$	European coastal waters	*Babin et al.* [2003b]
$a^*_{ph}(675)$			0.0199–0.0274		$m^2\ mg^{-1}$	Lake Chascomus	*Luis Perez et al.* [2011]
$a^*_{ph}(675)$			0.0288		$m^2\ mg^{-1}$	Lake Taihu	*Sun et al.* [2010]
$a^*_{ph}(675)$			0.018	0.005	$m^2\ mg^{-1}$	Lake Kasumigaura	*Yoshimura et al.* [2012]
$a^*_{ph}(676)$	0.002	0.042		0.009	$m^2\ mg^{-1}$	Long Island Sound	*Aurin et al.* [2010]
$a^*_{ph}(676)$	0.008	0.020	0.014		$m^2\ mg^{-1}$	15 boreal lakes	*Ylöstalo et al.* [2014]
$a^*_{ph}(670)$	0.007	0.157	0.040		$m^2\ mg^{-1}$	Lake Erie	*Binding et al.* [2008]
$a^*_{ph}(676)$			0.0171		$m^2\ mg^{-1}$	Onondaga Lake	*Perkins et al.* [2014]
$a^*_{ph}(676)$[a]	~0.004	~0.035			$m^2\ mg^{-1}$	European coastal waters	*Babin et al.* [2003b]

[a]Estimated from *Babin et al.* [2003b, Figure 6].

The specific absorption coefficient of phytoplankton showed variability across pigment concentrations (Figure 14). $a^*_{ph}(440)$ and $a^*_{ph}(675)$ varied by ~200% and ~150%, respectively, within the same basin on the same sampling date (i.e., Basin 2; Figures 14a and 14b), while $a^*_{ph}(620)$ showed less variability and a slight positive trend over increasing phycocyanin concentrations (Figure 14c). Previous studies in ocean waters have found $a^*_{ph}(\lambda)$ to decrease across increasing Chl-*a* concentrations, due to variations in pigment composition and pigment packaging [*Bricaud et al.*, 1995; *Bricaud*, 2004]. Although similar patterns were evident in Lake Balaton at 440 and 675 nm (Figures 14a and 14b), the relationships were not significant.

3.3.3. NAP Absorption

Figure 15 shows the absorption spectra for nonalgal particles for each basin and Kis-Balaton. $a_{NAP}(440)$ was 2–3 times higher in Kis-Balaton than in the lake basins, and was also significantly different between Basin 1 and Basins 2, 3, and 4 (Table 5). In general, marked variability was reported across the lake, with $a_{NAP}(350)$ ranging from up to 1.6 m^{-1} in Kis-Balaton to <0.1 m^{-1} in Basins 3 and 4 (Figure 15). Note that a small amount of residual pigment absorption can occasionally be observed in the spectra in the region of Chl-*a* absorption (~675 nm), due to incomplete bleaching. Residual pigment absorption in the a_{NAP} spectra propagated to an error of up to 5% in the calculated values of $a_{ph}(675)$, therefore this effect on $a_{ph}(\lambda)$ was considered minimal.

$a_{NAP}(\lambda)$ spectra followed a decreasing exponential shape, with a mean slope (S_{NAP}) of 0.0146 nm^{-1} (coefficient of variation = 26%), ranging from 0.011 to 0.025 nm^{-1} across all basins (Table 3). There were no significant differences in S_{NAP} found between the basins (Table 5). S_{NAP} generally declined with an increasing ratio of inorganic particulates, although the linear relationship was not significant ($R^2 = 0.0507$, $p > 0.1$, $n = 35$), with the greatest variability in S_{NAP} at lower ratios of PIM:POM (Figure 16a). S_{NAP} was negatively correlated to $a_{NAP}(440)$ for $a_{NAP}(440)$ <0.1 m^{-1} (Figure 16b). At TSM greater than ~10 mg L^{-1} and $a_{NAP}(440)$ greater than ~0.1 m^{-1}, S_{NAP} remained relatively constant (~0.01 nm^{-1}).

Scatterplots of $a_{NAP}(440)$ as a function of TSM and PIM are shown in Figure 17. When applying a linear regression with a null intercept to $a_{NAP}(440)$ as a function of TSM, a significantly lower slope (0.0069) exists

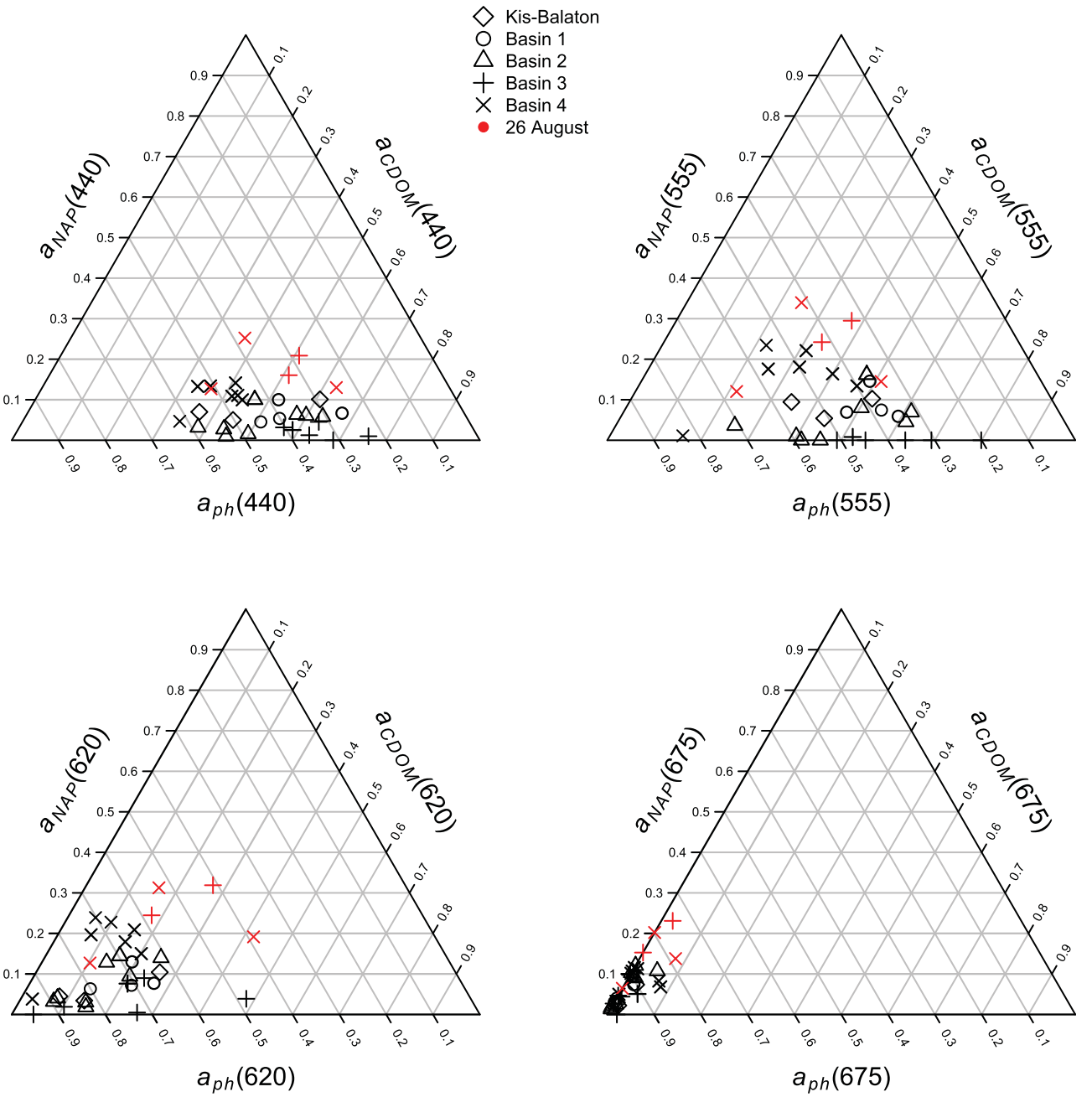

Figure 8. Ternary plot indicating absorption by phytoplankton (a_{ph}), nonalgal particles (a_{NAP}), and colored dissolved organic matter (a_{CDOM}) at (a) 440 nm, (b) 555 nm, (c) 620 nm, and (d) 675 nm. Unique symbols indicate the basin, and the sampling date 26 August is highlighted in red. Particulate absorption coefficients were measured in the laboratory by a dual beam spectrophotometer, and CDOM absorption was measured by spectrophotometry.

than that previously found in coastal waters (0.031) by *Babin et al.* [2003b] (Figure 17a) and thus presumably lower a_{NAP}*(440). The proportion of $a_{NAP}(440)$ to particulate absorption ($a_p(440)$) is additionally correlated with PIM (Figure 17b), indicating the strong influence by the mineral component of TSM toward nonalgal particle absorption.

4. Discussion

Using the ternary approach proposed by *Prieur and Sathyendranath* [1981], the relative contributions to the absorption budget were characterized in this study. At 675 nm, at least 70% of absorption is attributed to

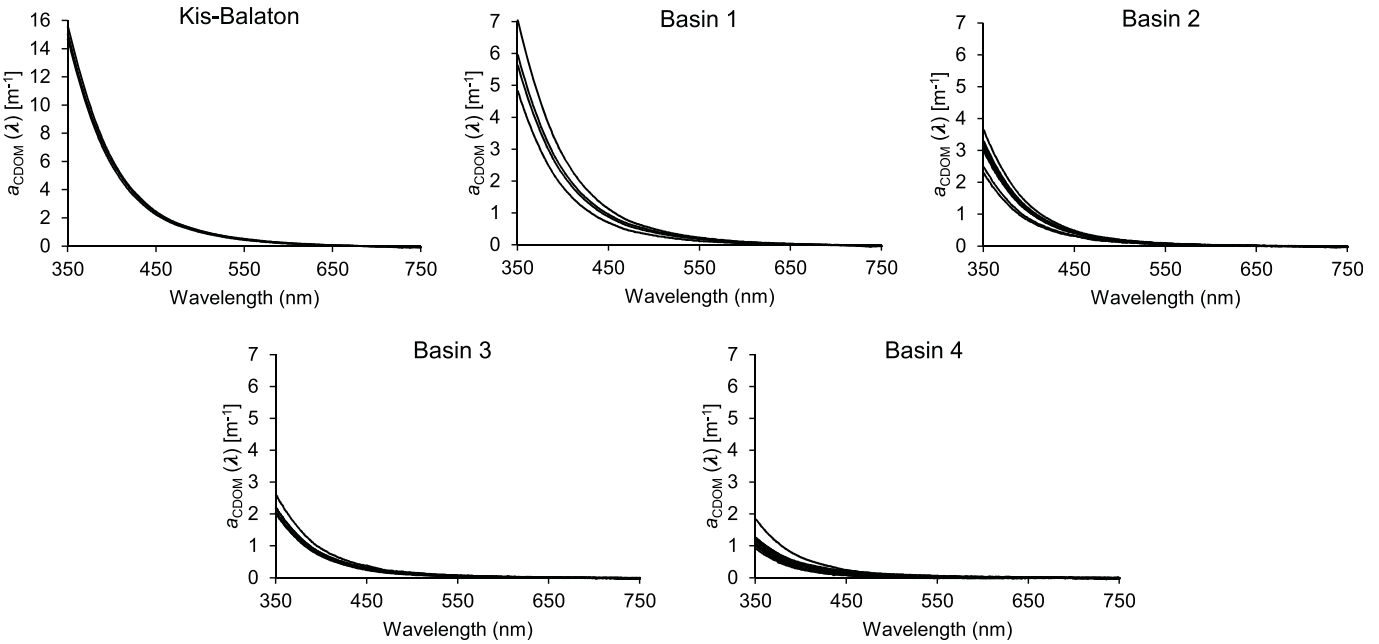

Figure 9. Spectra of absorption by color dissolved organic matter ($a_{CDOM}(\lambda)$) for all stations in Kis-Balaton and Lake Balaton by basin. Note the different *y* axis scale for Kis-Balaton.

phytoplankton, with up to 30% of absorption accounted for by NAP and CDOM (Figure 8). However, relative contributions were more variable in the blue portion of the spectrum (440 nm), where phytoplankton comprised between 20 and 70%, CDOM between 30 and 80% and NAP up to 30% of the absorption budget (Figure 8). In contrast, in coastal waters, it has been reported that NAP can form an even greater percentage of up to 80% of the nonwater absorption at 442 nm, although a similar contribution was observed from CDOM [*Babin et al.*, 2003b; *Tilstone et al.*, 2012]. In ocean waters, an approximately equal contribution to nonwater absorption has been measured from CDOM (40–50%) and phytoplankton (30–60%) at 440 nm [*Bricaud et al.*, 2010], although varying over a much narrower range than found in Lake Balaton. This

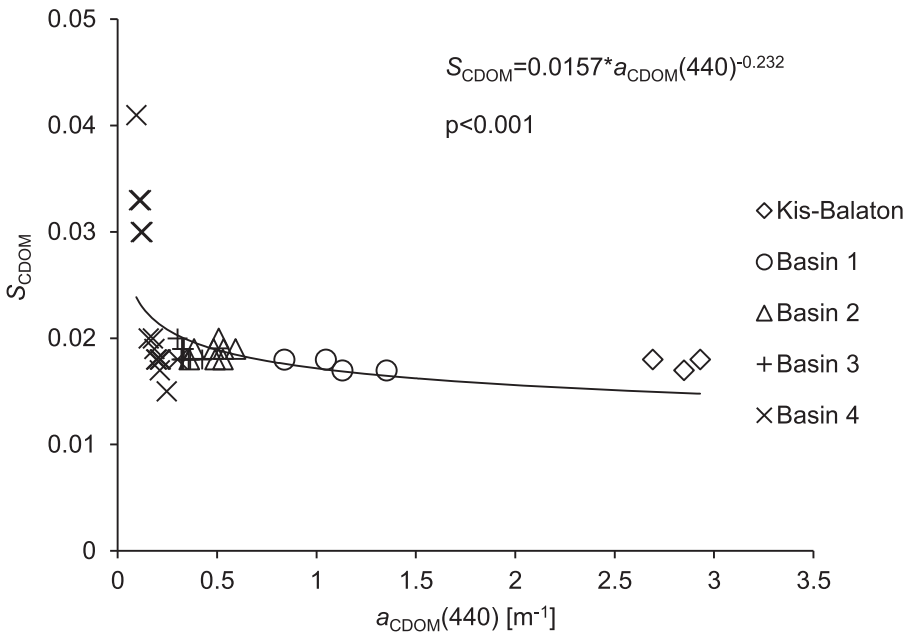

Figure 10. Plot of the slope of CDOM absorption coefficient (S_{CDOM}) as a function of CDOM absorption at 440 nm ($a_{CDOM}(440)$).

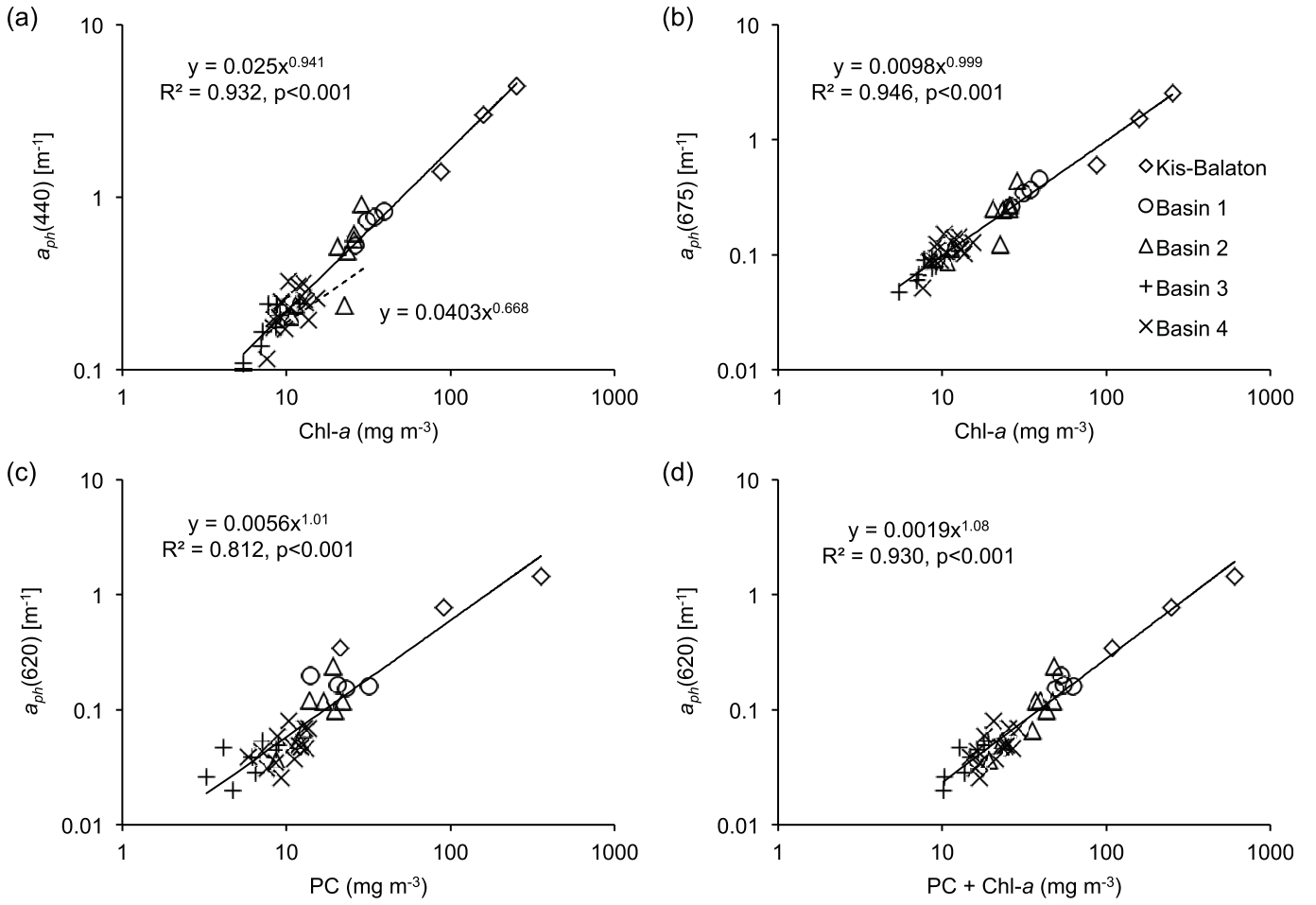

Figure 11. Scatterplots of the phytoplankton absorption coefficient (a_{ph}) at (a) 440 nm as a function of chlorophyll-*a* (Chl-*a*), (b) 675 nm as a function of Chl-*a*, (c) 620 nm as a function of phycocyanin (PC), and (d) 620 nm as a function of the summed pigments, PC + Chl-*a*. Chl-*a* results are by spectrophotometry, and PC results are a selected average of the results by spectrophotometry. Absorption coefficients were measured in the lab by spectrophotometry. Note axes are on logarithmic scale. Solid line is a regression curve by least squares fit, and the dashed line in Figure 11a is the fit from ocean waters in *Bricaud et al.* [1995].

indicates greater variations in the contributions to nonwater absorption than that reported for ocean waters, suggesting that inland waters may indeed exhibit more variability in optical properties than oceans. It is also important to note that the contribution of NAP to nonwater absorption in Lake Balaton is higher than that reported in ocean waters (e.g., up to 20% and typically below 10% at 440 nm in the South Pacific) [*Bricaud et al.*, 2010]. Contributions of CDOM and NAP were also relatively high at 620 nm (up to 48% and 32%, respectively) and 675 nm (up to 10% and 23%, respectively), wavelengths of particular interest for remote sensing retrievals of PC and Chl-*a* pigments. Similar instances were reported in some European coastal waters, where up to 60% of total absorption at the PC (620 nm) and Chl-*a* (665 nm) absorption peaks was due to particulate detritus, and a_{CDOM} occasionally contributed over 80% of absorption at 620 nm [*Babin et al.*, 2003b]. Similar findings were also reported in three South African reservoirs, where up to 60% and 30% of absorption was attributed to CDOM, while NAP contributed up to >90% and 60% at 620 and 675 nm, respectively [*Matthews and Bernard*, 2013]. The high contribution of NAP and CDOM at these wavelengths therefore must be considered in bio-optical models for pigment retrieval at these wavelengths.

A distinct gradient in optical properties was also observed along the trophic gradient of Lake Balaton. Basin 1 is phytoplankton-dominated water, while Basin 4 is mineral-dominated water, as shown by a decrease in the organic fraction of TSM from west to east, paralleled with a decrease in total phytoplankton biomass (Table 2). Total nonwater absorption ($a_p(\lambda)$ and $a_{CDOM}(\lambda)$) generally decreases from Basin 1 to 4 as the water progresses from phytoplankton-dominated to mineral-dominated. The significance of this is that

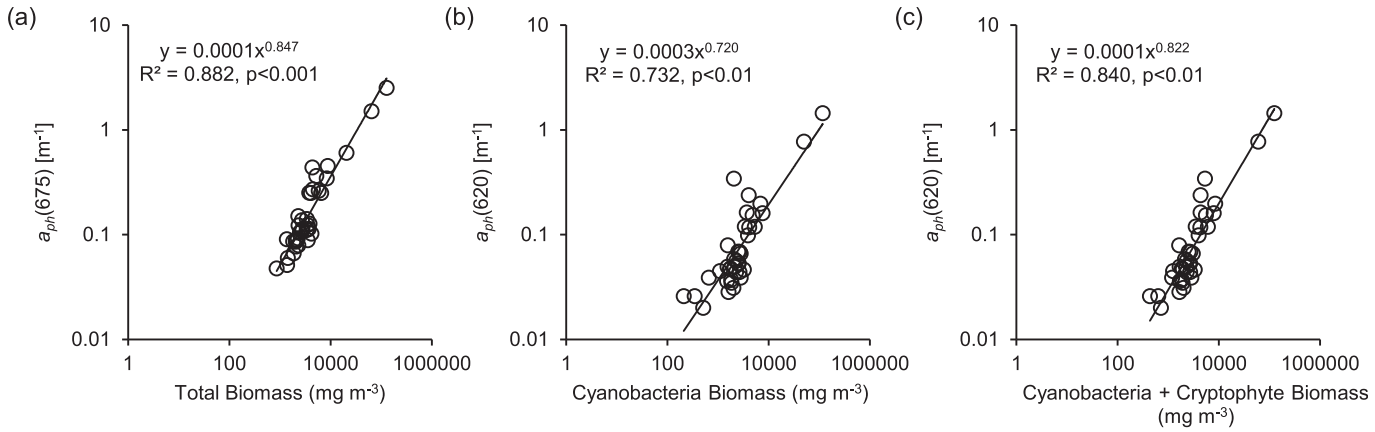

Figure 12. Regression of (a) total biomass, (b) cyanobacterial biomass, and (c) cyanobacteria and cryptophyte biomass against the absorption coefficient of phytoplankton (a_{ph}) at (a) 675 nm and (b and c) 620 nm, respectively. Absorption coefficients were measured in the laboratory by a dual beam spectrophotometer. Solid lines represent regression curves by least squares fit.

phytoplankton particles have different absorption properties than mineral particles. Phytoplankton pigments absorb strongly in the blue and red portion of the spectrum [*Mobley*, 1994], while inorganic particles have the highest absorption in the blue portion of the spectrum and near exponential decrease in absorption across the spectrum [*Babin et al.*, 2003b]. Therefore, this gradient in CDOM, phytoplankton, and mineral particles creates differences in both the quantity and quality of the underwater light field across Lake Balaton.

The IOPs in Lake Balaton generally show marked variability across the basins from the eutrophic western portion where biological particles dominate to the oligotrophic eastern basins with greater relative influence of minerogenic particles. As expected, Kis-Balaton and Lake Balaton had higher CDOM absorption than coastal ($a_{CDOM}(443) < 1$ m^{-1}) [*Babin et al.*, 2003b] or marine waters ($a_{CDOM}(375) = 0.06–4.2$ m^{-1}, although values >1 m^{-1} are rare) [*Bricaud et al.*, 1981], with levels markedly higher than hyperoligotrophic ocean waters ($a_{CDOM}(370)$ typically <0.04 m^{-1}) [*Morel et al.*, 2007]. However, mean CDOM absorption in Lake Balaton ($a_{CDOM}(440) = 0.58$ m^{-1}) was comparable with other shallow inland waters, with absorption coefficients higher than the oligotrophic Lake Superior [*Effler et al.*, 2010] or Lake Erie [*Binding et al.*, 2008], but lower than organic-rich lakes such as Lake Taihu and Chagan Lake in China [*Zhang et al.*, 2007, 2010; *Wang et al.*, 2011].

Comparisons of S_{CDOM} should be viewed cautiously because there is no commonly agreed standard wavelength range or method for calculating its value and approaches vary greatly in the literature. However, compared to studies with similar methods of calculation, mean S_{CDOM} for Lake Balaton (0.020 nm^{-1}) is generally higher than reported values for marine (0.014 ± 0.0032 nm^{-1}) [*Bricaud et al.*, 1981], European coastal waters (0.0176 ± 0.0020 nm^{-1}) [*Babin et al.*, 2003b] and the oligotrophic Lake Superior (0.0107–0.0134 nm^{-1}) [*Effler et al.*, 2010], but comparable to that reported for the shallow and eutrophic Oneida Lake (0.0186 nm^{-1}) [*Effler et al.*, 2012]. *Fichot and Benner* [2012] have shown that S_{CDOM} is a sensitive tracer of terrigenous dissolved organic carbon (DOC) in river-influenced ocean margins with lower values observed in more terrestrially influenced waters. The pool of DOC in Lake Balaton is likely to be dominated by allochthonous material, certainly in the western parts of the lake closer to the inflow of the Zala River where mean S_{CDOM} was lower (0.018 nm^{-1}).

This study also found $a_{ph}(675)$ to correlate linearly with the Chl-*a* concentration (Figure 11b), although large variability existed in the $a_{ph}(\lambda)$ parameter, especially at stations with higher concentrations of Chl-*a*. $a_{ph}(675)$ was further related to total phytoplankton biomass (Figure 12a), while $a_{ph}(620)$ varied linearly with the sum of cyanobacteria and cryptophyte biomass (Figures 12b and 12c). $a_{ph}(620)$ has not been specifically investigated in previous studies, and here we show a good relationship with PC concentrations, although a stronger correlation exists at this wavelength with summed PC and Chl-*a* pigments (Figure 11d). This wavelength (620 nm) is of importance in order to distinguish potentially harmful cyanobacteria blooms, and the correlation shown here for Lake Balaton is evidence for its future application to remote sensing algorithms for phycocyanin retrieval.

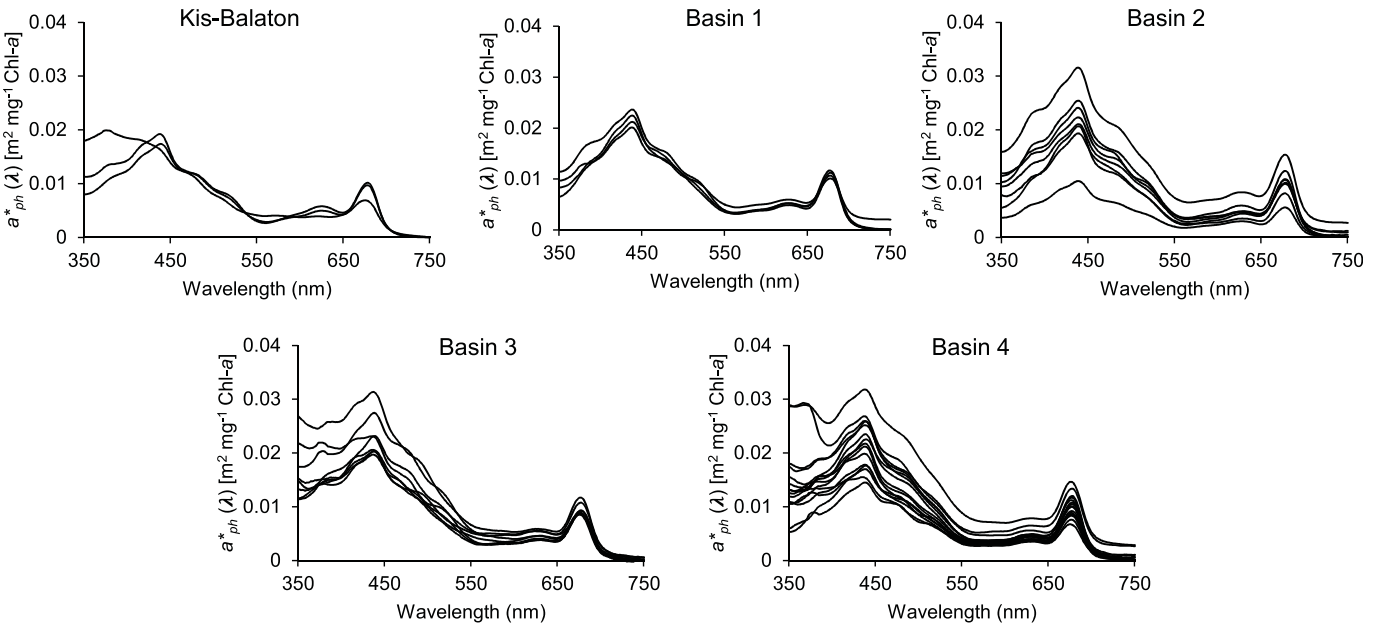

Figure 13. Spectra of mass-specific absorption by phytoplankton ($a^*_{ph}(\lambda)$) for all stations in Kis-Balaton and Lake Balaton by basin.

It is important to note that although there was a strong positive dependency of $a_{ph}(\lambda)$ on Chl-*a* (Figures 11a and 11b), this relationship was different from that observed in ocean waters, particularly at the 440 nm peak [*Bricaud et al*., 1995]. In Lake Balaton, there was greater absorption by phytoplankton at 440 nm per unit Chl-*a* than found in ocean waters in *Bricaud et al*. [1995], and this has also been reported in the English Channel [*Babin et al*., 2003b] and more recently, Lake Onondaga [*Perkins et al*., 2014] and three South African reservoirs [*Matthews and Bernard*, 2013]. However, the contrary was found in the North Sea and Western English Channel coastal waters, with slightly lower $a_{ph}(442)$ per unit Chl-*a* [*Tilstone et al*., 2012]. Given that the *Bricaud et al*. [1995] relationship was established over a narrower range of Chl-*a* (<30 mg m^{-3}), it is unsurprising that this relationship is different over the wider range of Chl-*a* concentrations found in Lake Balaton (~5–250 mg m^{-3}). It was suggested by *Babin et al*. [2003b] that the deviance from the *Bricaud et al*. [1995] relationship was likely a result of differences in phytoplankton cell size, given the widely accepted observation that oligotrophic waters are typically picoplankton-dominated while eutrophic waters are typically microplankton-dominated. In Lake Balaton, the dominant phytoplankton group (N-fixing cyanobacteria) was composed of mainly *Cylindrospermopsis raciborskii*, with *Aphanizomenon flos-aquae*, *Aphanizomenon issatschenkoi*, *Anabaena aphanizomenoides*, and *Planktothryx*

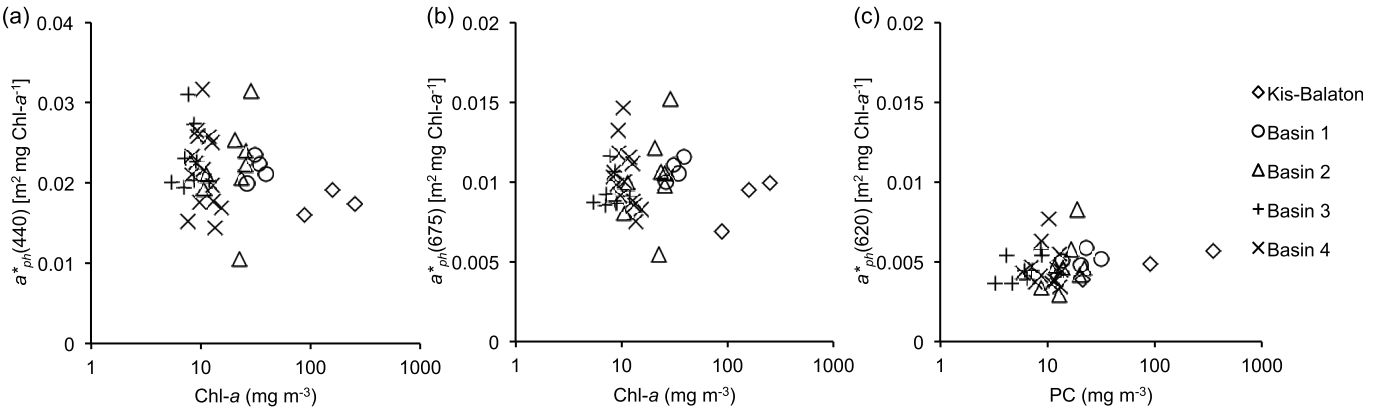

Figure 14. Variability of (a) $a^*_{ph}(440)$ and (b) $a^*_{ph}(675)$ over concentrations of chlorophyll-*a* (Chl-*a*) and (c) $a^*_{ph}(620)$ as a function of phycocyanin (PC) concentrations. Specific absorption coefficients were measured in the laboratory on a dual beam spectrophotometer, and PC and Chl-*a* results are from spectrophotometry. Note *x* axes are on log scale.

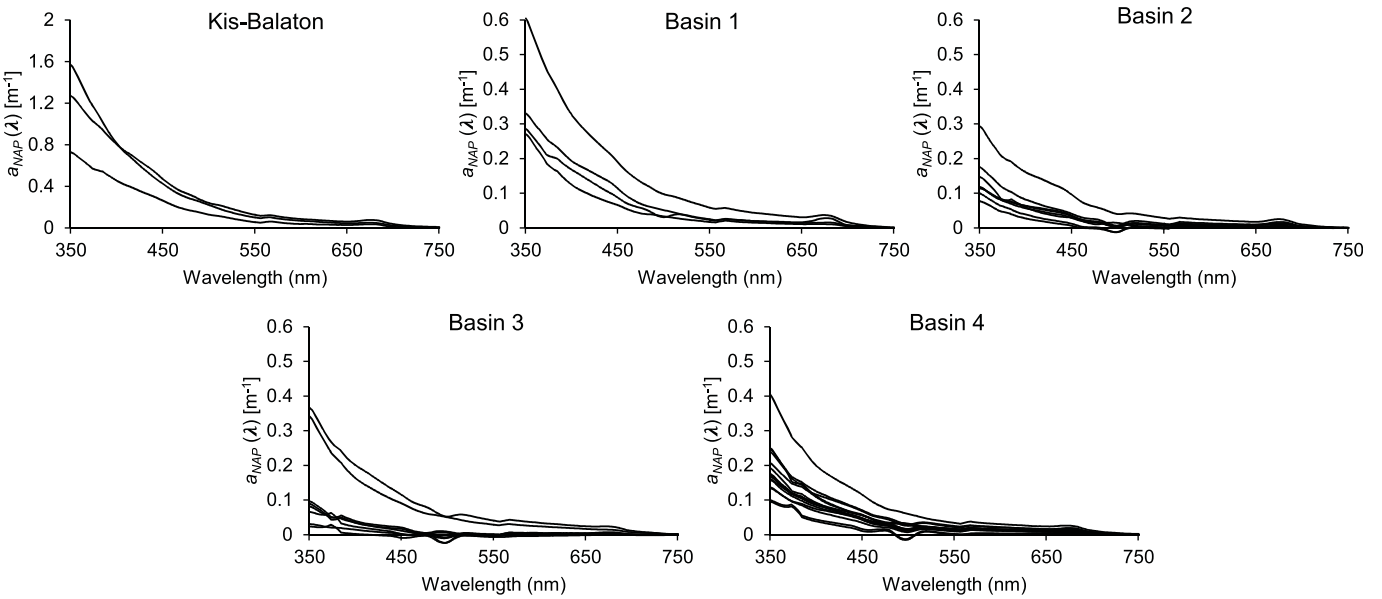

Figure 15. Spectra of absorption by nonalgal particles ($a_{NAP}(\lambda)$) for all stations in Kis-Balaton and Lake Balaton by basin. Note the different *y* axis maximum for Kis-Balaton.

agardhii also present. The cell size of these dominant cyanobacteria species was in the region of 100–200 μm, classifying this phytoplankton group as microplankton. Other large species were present in smaller numbers, including dinophytes (e.g., *Ceratium hirundinella*; 25–100 μm = microplankton) and large colonial diatoms (e.g., *Melosira granulate*, 1200 μm = microplankton), and the presence of these microplankton may account for the greater $a_{ph}(440)$ observed in Lake Balaton as compared to ocean waters.

The increased scatter found in the relationship between $a_{ph}(440)$ and Chl-*a* in Lake Balaton at ~10 mg m^{-3} Chl-*a* (Figure 11a) is also evident in coastal waters from the study by *Babin et al*. [2003b] (see Figure 7f therein), where it appears there is increased scatter in $a_{ph}(443)$ from ~0.3 to 10 mg m^{-3} Chl-*a*. In Lake Balaton, the greatest variation in $a_{ph}(440)$ was observed in Basins 3 and 4, and it is expected that this increased scatter is a result of variations in the phytoplankton community. Indeed, the eastern basins (Basins 3 and 4) comprised a more diverse phytoplankton community, with generally a greater range of community

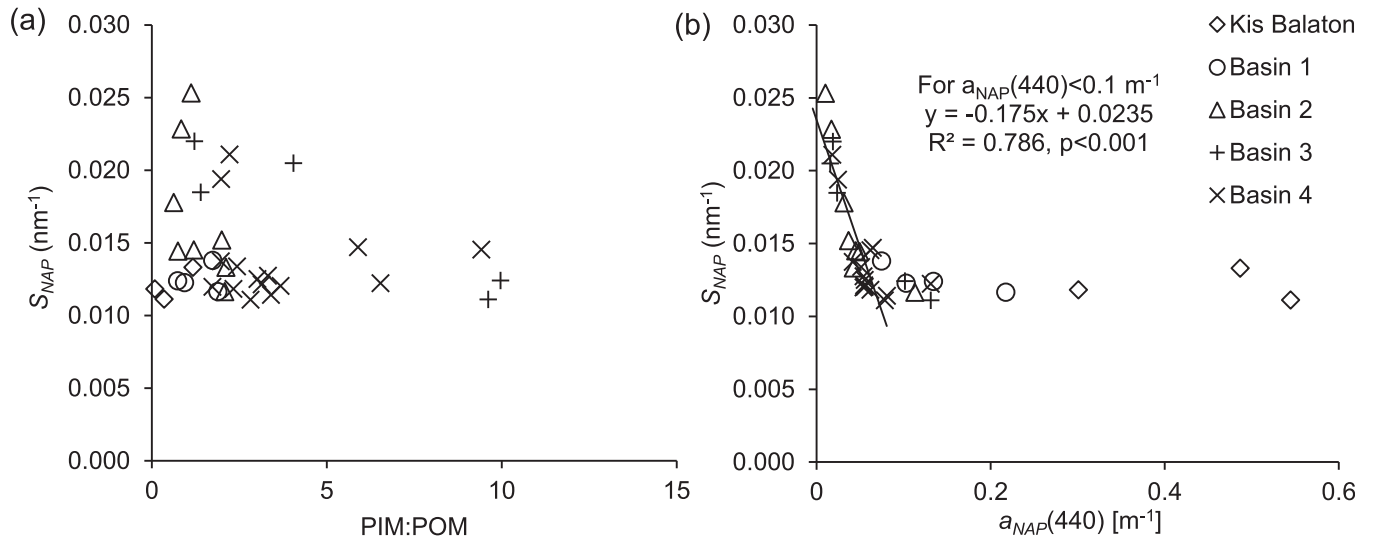

Figure 16. Scatterplots of S_{NAP} (the spectral slope of a_{NAP}) as a function of (a) the ratio of particulate inorganic to organic matter (PIM:POM) and (b) absorption by nonalgal particles at 440 nm ($a_{NAP}(440)$). The linear regression in Figure 16b is for $a_{NAP}(440)$ <0.1 m^{-1} only.

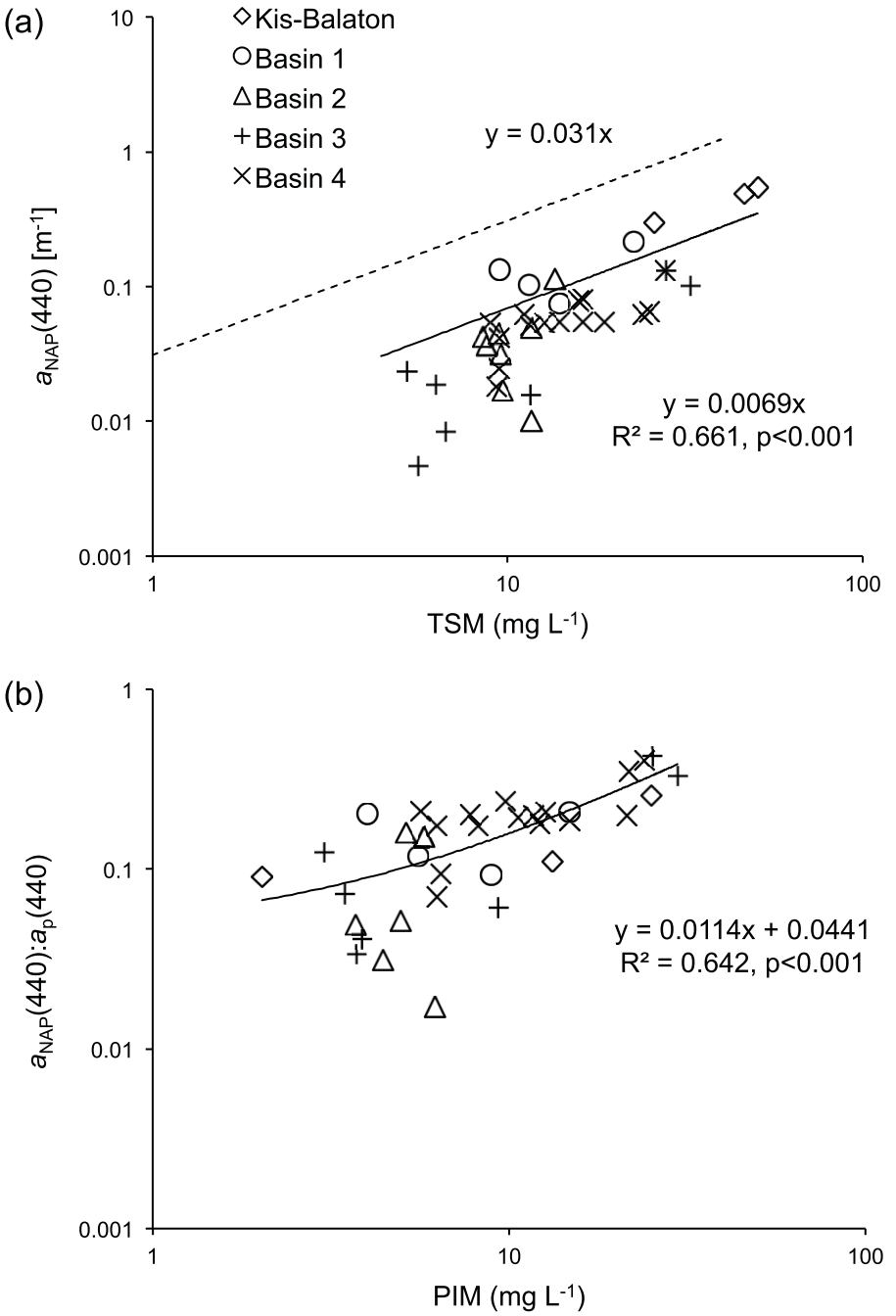

Figure 17. Correlation between (a) total suspended matter (TSM) and absorption by nonalgal particles ($a_{NAP}(440)$) and (b) particulate inorganic matter (PIM) and the proportion of absorption by nonalgal particles to absorption by particulate matter ($a_{NAP}(440)$:$a_p(440)$). In Figure 17a, dashed line is a linear regression with null intercept indicating the relationship found across the range of TSM in coastal waters in *Babin et al*. [2003b] ($a_{NAP}(440) = 0.31$*TSM), and the solid line is a linear regression with null intercept for Kis-Balaton and Lake Balaton. The solid line in Figure 17b is a linear regression.

composition between the stations as compared to the western basins where N-fixing cyanobacteria composed anywhere from 14 to 86% of the total biomass (Figure 4). This increased phytoplankton diversity, and thus increased variations in cell size, in the eastern basins would account for the greater variations in $a_{ph}(440)$ per unit Chl-*a* that were observed in this portion of Lake Balaton.

The Chl-*a*-specific absorption coefficient ($a^*_{ph}(\lambda)$) has been identified as a major source of uncertainty in accurately retrieving Chl-*a* in turbid productive waters [*Dall'Olmo and Gitelson*, 2006]. The mean $a^*_{ph}(440)$

ranged from 0.017 to 0.023 m^2 mg^{-1} across Kis-Balaton and the four lake basins. In comparison, $a^*_{ph}(443)$ varies over a much broader range in ocean (~0.01–0.18 m^2 mg^{-1}; from Figure 1 in *Bricaud et al.* [1995]) and coastal waters (~0.008–0.10 m^2 mg^{-1}; from *Babin et al.* [2003b, Figure 6]). However, measured $a^*_{ph}(440)$ in Lake Balaton is within the range measured in three small oligotrophic to hypereutrophic reservoirs (0.005–0.084 m^2 mg^{-1}) [*Matthews and Bernard*, 2013]. Comparable $a^*_{ph}(440)$ were also reported in Lake Kasumigaura (0.026 m^2 mg^{-1}) [*Yoshimura et al.*, 2012], while higher coefficients were reported in Lake Erie (0.086 m^2 mg^{-1}) [*Binding et al.*, 2008] and Onondaga Lake (0.035 m^2 mg^{-1}) [*Perkins et al.*, 2014]. Mean $a^*_{ph}(675)$ values varied over a narrow range across the four basins and Kis-Balaton (0.0088–0.011 m^2 mg^{-1}). The mean $a^*_{ph}(675)$ in Balaton is on the lower end of the range reported for ocean waters (~0.005–0.06 m^2 mg^{-1}) [*Bricaud et al.*, 1995], and most similar to the coastal waters in the Baltic and Adriatic Seas [*Babin et al.*, 2003b] or Long Island Sound (median $a^*_{ph}(676) = 0.010$ m^2 mg^{-1}) [*Aurin et al.*, 2010]. While $a^*_{ph}(675)$ in Lake Balaton falls on the low end of the range for highly turbid lakes such as the hypereutrophic Lake Chascomus, Argentina ($a^*_{ph}(675) = 0.0199–0.0274$ m^2 mg^{-1}) [*Luis Perez et al.*, 2011] and eutrophic Lake Taihu, China (mean $a^*_{ph}(675) = 0.0288$ m^2 mg^{-1}) [*Sun et al.*, 2010], it was similar to the alkaline hypereutrophic to mesotrophic conditions in Onondaga Lake, New York, USA (mean $a^*_{ph}(676) = 0.0171$ m^2 mg^{-1}) [*Perkins et al.*, 2014].

Previous studies document that $a^*_{ph}(\lambda)$ decreases from oligotrophic to eutrophic waters, due to the "pigment package effect" and changes in species composition and thus pigmentation [*Bricaud et al.*, 1995]. However, in Lake Balaton, there was no clear trend of decreasing $a^*_{ph}(440)$ or $a^*_{ph}(675)$ across increasing concentrations of Chl-*a* (Figures 14a and 14b), although any trend in $a^*_{ph}(\lambda)$ may be unclear in this study simply due to the relatively small sample size of 38 stations or the relatively small Chl-*a* gradient in Lake Balaton. Similarly, $a^*_{ph}(620)$ showed a narrow range across the basins (~0.002–0.008 m^2 mg^{-1}), and a general trend of increasing $a^*_{ph}(620)$ across increasing phycocyanin concentrations (Figure 14b). It has recently been suggested that $a^*_{ph}(\lambda)$ varies greatly with phytoplankton species composition; for example, in Lake Taihu $a^*_{ph}(\lambda)$ increased with the succession from chlorophytes to cyanophytes [*Zhang et al.*, 2012]. Lake Balaton was dominated by cyanobacteria during the sampling period, which is possibly why no significant changes in $a^*_{ph}(\lambda)$ were observed between basins. However, there were variations in phytoplankton community composition within the nondominant functional groups, including a greater percentage of chlorophytes, dinophytes, and diatoms (heterokontophytes) in Basins 3 and 4 (Figure 4). In particular, the slightly greater abundance of microplankton in Basin 3 (96%, compared to 87–95% in Basins 1, 2, and 4), including dinoflagellates (*Gymnodinium* sp., 25 μm), diatoms (*Synedra acus* v. rad, 110 μm) and chlorophytes (*Schroederia robusta*, 80 μm; *Staurastrum paradoxum*, 40 μm), may explain the low mean $a^*_{ph}(675)$ measured in this basin (0.0094 m^2 mg^{-1}). Larger cells are subject to a greater package effect and thus decreased absorption efficiency. Thus, the observed variations in $a^*_{ph}(\lambda)$ may be a result of changes in pigment packaging within the different cell types due to variations in cell size with the change in phytoplankton community composition.

The phytoplankton absorption peak in the UV in Basins 3 and 4 corresponds with decreased CDOM absorption in these eastern basins (mean $a_{CDOM}(440)$ 0.34 and 0.18 m^{-1}, respectively), compared with the CDOM absorption in the western basins (mean $a_{CDOM}(440)$ ranges from 0.48 to 2.82 m^{-1}). As CDOM absorbs strongly in the lower wavelengths (see Figure 9), it may serve as a UV protectant for phytoplankton and other organisms. It is possible that the cyanobacteria in the eastern basins of Lake Balaton are compensating for this decrease in CDOM by producing a pigment to absorb harmful UV rays. In a recent study on the Florida Keys, phytoplankton were found to produce mycosporine-like amino acids (MAAs) to absorb ultraviolet (UV) light, with a peak in a_{ph} at ~315–360 nm, to compensate for low CDOM absorption [*Ayoub et al.*, 2012]. There are inchoative results of MAA production by *Cylindrospermopsis raciborskii* in Lake Balaton (A. W. Kovács, personal communication, 2015), and many marine cyanobacteria species have been documented to produce MAAs [*Sinha et al.*, 2007]. An earlier study also details the presence of UV-screening compounds in terrestrial cyanobacteria mats, including MAAs and scytonemin [*Cockell and Knowland*, 1999]. In freshwater lakes, the literature is scarce, with *Microcystis aeruginosa* as the only documented cyanobacteria species found to produce MAAs [*Liu et al.*, 2004]. It is therefore possible that one of the most dominant cyanobacteria in Lake Balaton are producing MAAs or similar photoprotective pigments in response to UV stress in the eastern basins where there are lower concentrations of CDOM.

The SIOPs varied greatly from west to east across Lake Balaton, principally based on the distance from the main source of nutrients and organic matter, the Zala River. Each station was assigned a distance from the

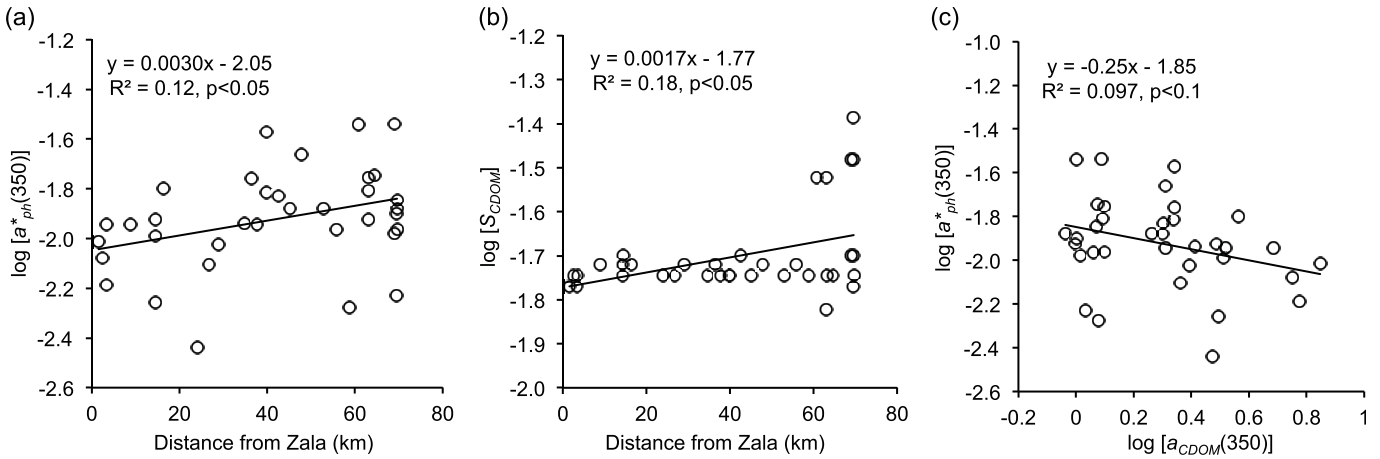

Figure 18. Variation of (a) log ($a^*_{ph}(350)$) ($m^2\ mg^{-1}$) and (b) log (S_{CDOM}) (nm^{-1}) over increasing distance from the Zala River inflow, and (c) relationship between log($a^*_{ph}(350)$) ($m^2\ mg^{-1}$) and log ($a_{CDOM}(350)$) (m^{-1}).

Zala River, and significant differences ($p < 0.05$) were found where none were previously observed using the four basin designations (Figure 18). $a^*_{ph}(350)$ was found to increase with increasing distance from the Zala River over a decreasing CDOM gradient (Figures 18a and 18c). Given that a single species comprised the dominant phytoplankton over the study period, it is theorized that the change in a^*_{ph} in the UV portion of the spectrum is linked to the variable production of photoprotective pigments. Additionally, a significant change in S_{CDOM} was measured with increasing distance from the Zala River (Figure 18b). The western basins have a larger terrestrial input to CDOM, given the proximity to the river, and this is reflected in the lower values of S_{CDOM}. It is important to note that this positive correlation is driven by a small number of stations >60 km from the Zala River, and a subsequent in-depth spatial investigation of S_{CDOM} would clarify this relationship. In bio-optical models for retrieval of IOPs and pigments from remote sensing, the $a_{CDOM}(\lambda)$ absorption spectrum is often derived from an assumed or estimated S_{CDOM} [*Lee et al*., 2002; *Mishra et al*., 2013; *Li et al*., 2013, 2015]. As such, S_{CDOM} may be a prime source of error in the parameterization of analytical models, with further propagation of errors to retrieved pigment concentrations.

Lake Balaton is often characterized by high and heterogeneous concentrations of suspended minerals due to the wind-induced resuspension of dolomite limestone bottom sediments [*Tyler et al*., 2006], with lake mean PIM concentrations comprising over 70% of TSM. Most of the variability in TSM concentrations in this study was explained by PIM (57%), and significantly more so if the three Kis-Balaton stations are excluded (96%) (Kis-Balaton is dominated by phytoplankton, with POM comprising up to 92% of the TSM at station KB2). The proportion of $a_{NAP}(\lambda)$ was also significantly correlated with PIM, demonstrating the large contribution from inorganic matter to nonalgal particulate absorption (Figure 17). A study on mineral absorption found that mineral absorption in the Irish Sea decreases from blue to red, with a slight increase between 450 and 550 nm [*Bowers and Binding*, 2006]. This does not seem to be the case in Lake Balaton, and in fact, the spectra sometimes show a slight dip in this wavelength range. This can largely be explained by the difference in sediment types, specifically the siliceous sediments of the Irish Sea [*Bryant et al*., 1996] contrasting with the dolomitic sediments of Lake Balaton [*Tyler et al*., 2006].

The slope of the $a_{NAP}(\lambda)$ curve (S_{NAP}) was similar across all basins, with a mean value of $0.015 \pm 0.004\ nm^{-1}$. Other studies have reported similarly narrow ranges of S_{NAP}, however mean S_{NAP} in Lake Balaton was distinctly higher than that reported in ocean (0.0094 ± 0.0018 [*Bricaud et al*., 2010] and 0.011 ± 0.0025 [*Bricaud et al*., 1998]) or coastal waters [*Babin et al*., 2003b; *Bowers and Binding*, 2006]. Comparable values were reported for the turbid waters of western Lake Erie [*Peng and Effler*, 2013], although maximum S_{NAP} values in Lake Balaton were higher. *Babin et al*. [2003b] hypothesized that the observed variations in S_{NAP} in coastal waters were a result of the differences in the proportion of mineral versus organic matter. Differences related to NAP composition were found in this study, with lower mean S_{NAP} reported in Kis-Balaton where the highest proportion of organic matter was measured (46–92% POM), while higher mean values were reported in Basins 2 and 3 where PIM comprised up to 90% of TSM (Basin 3). S_{NAP} also generally declined with an increasing ratio of inorganic particulates, but followed a distinctly linear decreasing pattern with

$a_{NAP}(440)$ for values of $a_{NAP}(440) < 0.1$ m^{-1} (Figure 16). *Bricaud et al.* [2010] also found a decrease in S_{NAP} over a low range of $a_{NAP}(440)$ in ocean waters (<0.05 m^{-1}), which they attributed to the variable abundance and nature of organic particles comprising the NAP pool (e.g., weakly colored versus colored particles). It is likely that the differing nature of organic particles which make up the NAP in Lake Balaton also contributes to the observed variations in S_{NAP}, particularly for low levels of TSM (<10 mg L^{-1}) and $a_{NAP}(440)$ (<0.1 m^{-1}).

Another potential source of variability in the optical properties of Lake Balaton is the change in the composition and size distribution of particles, as often occurs during resuspension events. The absorption measured at stations sampled on 26 August 2010 in this study indicated a marked difference in contributions from phytoplankton, nonalgal particles and CDOM to total absorption (Figure 8). The mean wind speed on 26 August at Siófok was 3.6 m s^{-1}, which is higher than the daily averages from the other seven sampling dates (Table 1). Additionally, the maximum wind speed on 26 August was 5.1 m s^{-1}, with an even greater maximum of 13.6 m s^{-1} reported on the previous day (25 August). As the generally accepted threshold for turbulent mixing in shallow lakes is 4 m s^{-1} [*Hunter et al.*, 2008], it is likely that the water column was affected by substantial resuspension of sediments on 26 August. This difference in sampling conditions may explain some of the variability in the (S)IOPs seen in this study, as wind-driven resuspension of sediments has been shown to cause significant increases in light absorption, scattering and attenuation particularly in shallow inland or coastal waters [*Zhang et al.*, 2006; *Verspecht and Pattiaratchi*, 2010; *Liu et al.*, 2014]. Due to highly variable winds across Lake Balaton, both temporally and spatially, future study should include anemometer readings taken alongside the optical measurements at each station in order to investigate this effect further. There is also a lag time effect from weather conditions from the previous day, which should be considered when interpreting the effect on optical properties.

In summary, the IOPs in Lake Balaton show distinct spatial variability, with decreasing absorption coefficients across a decreasing trophic gradient of Chl-*a* and phytoplankton biomass. a_{NAP} was significantly correlated with PIM, which indicates the strong influence of mineral particles on nonwater absorption in Lake Balaton. Specific phytoplankton absorption ($a^*_{ph}(675)$) was variable across Chl-*a* concentrations, with no clear trend across the basins, likely due to the dominance of one cyanobacteria species across the lake (*Cylindrospermopsis raciborskii*). However, significant differences were reported in $a^*_{ph}(350)$ and S_{CDOM} over increasing distance from the Zala River and a decreasing CDOM gradient. This is likely to be linked to the variable production of photoprotective pigments (i.e., MAAs), as opposed to variations in the phytoplankton community composition. While this study was suitable for demonstrating a convincing investigation of spatial variability in (S)IOPs in Lake Balaton, further investigation into seasonal variations is pertinent. With regard to the wider implications to remote sensing, bio-optical models for inversion of constituents such as Chl-*a* must consider the full range of values for (S)IOPs in that water body in order to avoid significant uncertainties in the retrieved values. This has implications for algorithm applications in large shallow lakes with variable biogeochemistry across basins, such as Lake Balaton, and calls into question whether a single algorithm for constituent extraction is suitable across the entire lake. Large lakes with variable biogeochemistry may require basin-specific remote sensing algorithms for accurate parameter retrieval [e.g., *Campbell et al.*, 2011]. This research will furthermore contribute toward progressing bio-optical models using absorption and scattering measurements to improve remote sensing retrieval in optically complex waters.

Acknowledgments

Wind speed data were measured by automatic stations established by predecessor in the title of Lake Balaton Development Coordination Agency and operated by the Central-Transdanubian Water Directorate. Absorption and biogeochemical data can be found on the LIMNADES database (http://www.lochs-ustir.org/). Cell biomass data are provided by the corresponding author upon request. The AC-S and DH4 (WET Labs Inc.) and the CTD (Sea-Bird Electronics) equipment for this work were provided by NERC Field Spectroscopy Facility (Edinburgh), as part of loan ref EU10-03. Other funding was provided by TÁMOP-4.2.2.A-11/1/KONV-2012-0038 project in part for evaluation and processing of field data. Field assistance on Lake Balaton was provided by Eszter Zsigmond and Géza Dobos and lab assistance was provided by Terézia Horváth and Erika Kozma. Cell size data were provided by Claire Neil. The authors would like to particularly acknowledge the late Mátyás Présing, who contributed to this research and was a valued colleague and friend.

References

Astoreca, R., D. Doxaran, K. Ruddick, V. Rousseau, and C. Lancelot (2012), Influence of suspended particle concentration, composition and size on the variability of inherent optical properties of the Southern North Sea, *Cont. Shelf Res.*, *35*, 117–128, doi:10.1016/j.csr.2012.01.007.

Aurin, D. A., H. M. Dierssen, M. S. Twardowski, and C. S. Roesler (2010), Optical complexity in Long Island Sound and implications for coastal ocean color remote sensing, *J. Geophys. Res.*, *115*, C07011, doi:10.1029/2009JC005837.

Ayoub, L. M., P. Hallock, P. G. Coble, and S. S. Bell (2012), MAA-like absorbing substances in Florida Keys phytoplankton vary with distance from shore and CDOM: Implications for coral reefs, *J. Exp. Mar. Biol. Ecol.*, *420*, 91–98, doi:10.1016/j.jembe.2012.03.026.

Babin, M., A. Morel, V. Fournier-Sicre, F. Fell, and D. Stramski (2003a), Light scattering properties of marine particles in coastal and open ocean waters as related to the particle mass concentration, *Limnol. Oceanogr. Methods*, *48*(2), 843–859.

Babin, M., D. Stramski, G. Ferrari, H. Claustre, A. Bricaud, G. Obolensky, and N. Hoepffner (2003b), Variations in the light absorption coefficients of phytoplankton, nonalgal particles, and dissolved organic matter in coastal waters around Europe, *J. Geophys. Res.*, *108*(C7), 3211, doi:10.1029/2001JC000882.

Barlow, R., D. Cummings, and S. Gibb (1997), Improved resolution of mono- and divinyl chlorophylls a and b and zeaxanthin and lutein in phytoplankton extracts using reverse phase C-8 HPLC, *Mar. Ecol. Prog. Ser.*, *161*, 303–307, doi:10.3354/meps161303.

Bertilsson, S., and L. Tranvik (2000), Photochemical transformation of dissolved organic matter in lakes, *Limnol. Oceanogr.*, *45*(4), 753–762.
Binding, C. E., J. H. Jerome, R. P. Bukata, and W. G. Booty (2008), Spectral absorption properties of dissolved and particulate matter in Lake Erie, *Remote Sens. Environ.*, *112*(4), 1702–1711, doi:10.1016/j.rse.2007.08.017.
Blache, U., T. Jakob, W. Su, and C. Wilhelm (2011), The impact of cell-specific absorption properties on the correlation of electron transport rates measured by chlorophyll fluorescence and photosynthetic oxygen production in planktonic algae, *Plant Physiol. Biochem.*, *49*(8), 801–808, doi:10.1016/j.plaphy.2011.04.010.
Bowers, D., and C. Binding (2006), The optical properties of mineral suspended particles: A review and synthesis, *Estuarine Coastal Shelf. Sci.*, *67*(1–2), 219–230, doi:10.1016/j.ecss.2005.11.010.
Bricaud, A. (2004), Natural variability of phytoplanktonic absorption in oceanic waters: Influence of the size structure of algal populations, *J. Geophys. Res.*, *109*, C11010, doi:10.1029/2004JC002419.
Bricaud, A., A. Morel, and L. Prieur (1981), Absorption by dissolved organic-matter of the sea (yellow substance) in the UV and visible domains, *Limnol. Oceanogr.*, *26*(1), 43–53.
Bricaud, A., M. Babin, A. Morel, and H. Claustre (1995), Variability in the chlorophyll-specific absorption-coefficients of natural phytoplankton—Analysis and parameterization, *J. Geophys. Res.*, *100*(C7), 13,321–13,332, doi:10.1029/95JC00463.
Bricaud, A., A. Morel, M. Babin, K. Allali, and H. Claustre (1998), Variations of light absorption by suspended particles with chlorophyll a concentration in oceanic (case 1) waters: Analysis and implications for bio-optical models, *J. Geophys. Res.*, *103*(C13), 31,033–31,044, doi:10.1029/98JC02712.
Bricaud, A., M. Babin, H. Claustre, J. Ras, and F. Tieche (2010), Light absorption properties and absorption budget of Southeast Pacific waters, *J. Geophys. Res.*, *115*, C08009, doi:10.1029/2009JC005517.
Bryant, R., A. Tyler, D. Gilvear, P. McDonald, I. Teasdale, J. Brown, and G. Ferrier (1996), A preliminary investigation into the spectral characteristics of inter-tidal estuarine sediments, *Int. J. Remote Sens.*, *17*(2), 405–412.
Campbell, G., S. R. Phinn, A. G. Dekker, and V. E. Brando (2011), Remote sensing of water quality in an Australian tropical freshwater impoundment using matrix inversion and MERIS images RID A-1321-2008, *Remote Sens. Environ.*, *115*(9), 2402–2414, doi:10.1016/j.rse.2011.05.003.
Ciavatta, S., R. Torres, V. Martinez-Vicente, T. Smyth, G. Dall'Olmo, L. Polimene, and J. I. Allen (2014), Assimilation of remotely-sensed optical properties to improve marine biogeochemistry modelling, *Prog. Oceanogr.*, *127*, 74–95, doi:10.1016/j.pocean.2014.06.002.
Cockell, C. S., and J. Knowland (1999), Ultraviolet radiation screening compounds, *Biol. Rev. Cambridge Philos. Soc.*, *74*(3), 311–345, doi:10.1017/S0006323199005356.
Dall'Olmo, G., and A. Gitelson (2005), Effect of bio-optical parameter variability on the remote estimation of chlorophyll-a concentration in turbid productive waters: Experimental results, *Appl. Opt.*, *44*(3), 412–422, doi:10.1364/AO.44.000412.
Dall'Olmo, G., and A. A. Gitelson (2006), Effect of bio-optical parameter variability and uncertainties in reflectance measurements on the remote estimation of chlorophyll-a concentration in turbid productive waters: Modeling results, *Appl. Opt.*, *45*(15), 3577–3592, doi:10.1364/AO.45.003577.
Dera, J., and B. Wozniak (2010), Solar radiation in the Baltic Sea, *Oceanologia*, *52*(4), 533–582, doi:10.5697/oc.52-4.533.
Effler, S. W., M. Perkins, F. Peng, C. Strait, A. D. Weidemann, and M. T. Auer (2010), Light-absorbing components in Lake Superior, *J. Great Lakes Res.*, *36*(4), 656–665, doi:10.1016/j.jglr.2010.08.001.
Effler, S. W., C. M. Strait, M. Perkins, and D. M. O'Donnell (2012), Optical characterization and tests of closure for Oneida Lake, New York, USA, *Inland Waters*, *2*(4), 211–228, doi:10.5268/IW-2.4.503.
Fichot, C. G., and R. Benner (2012), The spectral slope coefficient of chromophoric dissolved organic matter (S275-295) as a tracer of terrigenous dissolved organic carbon in river-influenced ocean margins, *Limnol. Oceanogr. Methods*, *57*(5), 1453–1466, doi:10.4319/lo.2012.57.5.1453.
Gilerson, A. A., A. A. Gitelson, J. Zhou, D. Gurlin, W. Moses, I. Ioannou, and S. A. Ahmed (2010), Algorithms for remote estimation of chlorophyll-a in coastal and inland waters using red and near infrared bands, *Opt. Express*, *18*(23), 24,109–24,125, doi:10.1364/OE.18.024109.
Gordon, H., O. Brown, and M. Jacobs (1975), Computed relationships between inherent and apparent optical-properties of a flat homogeneous ocean, *Appl. Opt.*, *14*(2), 417–427, doi:10.1364/AO.14.000417.
Herodek, S. (1986), Phytoplankton changes during eutrophication and P and N metabolism, in *Modeling and Managing Shallow Lake Eutrophication: With Application to Lake Balaton*, vol. 2, edited by L. Somlyódy and G. van Straten, pp. 183–204, Springer, Berlin.
Horváth, H., A. W. Kovács, C. Riddick, and M. Présing (2013), Extraction methods for phycocyanin determination in freshwater filamentous cyanobacteria and their application in a shallow lake, *Eur. J. Phycol.*, *48*(3), 278–286, doi:10.1080/09670262.2013.821525.
Huang, C., X. Chen, Y. Li, H. Yang, D. Sun, J. Li, C. Le, L. Zhou, M. Zhang, and L. Xu (2015), Specific inherent optical properties of highly turbid productive water for retrieval of water quality after optical classification, *Environ. Earth Sci.*, *73*(5), 1961–1973, doi:10.1007/s12665-014-3548-3.
Hunter, P. D., A. N. Tyler, N. J. Willby, and D. J. Gilvear (2008), The spatial dynamics of vertical migration by *Microcystis aeruginosa* in a eutrophic shallow lake: A case study using high spatial resolution time-series airborne remote sensing, *Limnol. Oceanogr. Methods*, *53*(6), 2391–2406.
Hunter, P. D., A. N. Tyler, L. Carvalho, G. A. Codd, and S. C. Maberly (2010), Hyperspectral remote sensing of cyanobacterial pigments as indicators for cell populations and toxins in eutrophic lakes, *Remote Sens. Environ.*, *114*(11), 2705–2718, doi:10.1016/j.rse.2010.06.006.
IOCCG (2000), Remote sensing of ocean colour in coastal, and other optically-complex, waters, in *Reports of the International Ocean-Colour Coordinating Group, IOCCG Rep. 3*, 137 pp., Darmouth, Nova Scotia, Canada.
Iwamura, T., H. Nagai, and S. Ichimura (1970), Improved methods for determining contents of chlorophyll, protein, ribonucleic acid, and deoxyribonucleic acid in planktonic populations, *Int. Rev. Hydrobiol. Hydrogr.*, *55*(1), 131–147, doi:10.1002/iroh.19700550106.
Jolliff, J. K., J. C. Kindle, B. Penta, R. Helber, Z. Lee, I. Shulman, R. Arnone, and C. D. Rowley (2008), On the relationship between satellite-estimated bio-optical and thermal properties in the Gulf of Mexico, *J. Geophys. Res.*, *113*, G01024, doi:10.1029/2006JG000373.
Kirk, J. (1994), *Light and Photosynthesis in Aquatic Ecosystems*, Cambridge Univ. Press, Cambridge, U. K.
Kutser, T., L. Metsamaa, N. Strombeck, and E. Vahtmae (2006), Monitoring cyanobacterial blooms by satellite remote sensing, *Estuarine Coastal Shelf Sci.*, *67*(1–2), 303–312, doi:10.1016/j.ecss.2005.11.024.
Lee, Z. P., K. L. Carder, and R. A. Arnone (2002), Deriving inherent optical properties from water color: A multiband quasi-analytical algorithm for optically deep waters, *Appl. Opt.*, *41*(27), 5755–5772, doi:10.1364/AO.41.005755.
Lee, Z. P., et al. (2011), An assessment of optical properties and primary production derived from remote sensing in the Southern Ocean (SO GasEx), *J. Geophys. Res.*, *116*, C00F03, doi:10.1029/2010JC006747.
Leymarie, E., D. Doxaran, and M. Babin (2010), Uncertainties associated to measurements of inherent optical properties in natural waters, *Appl. Opt.*, *49*(28), 5415–5436, doi:10.1364/AO.49.005415.

Li, L., L. Li, K. Song, Y. Li, L. P. Tedesco, K. Shi, and Z. Li (2013), An inversion model for deriving inherent optical properties of inland waters: Establishment, validation and application, *Remote Sens. Environ.*, *135*, 150–166, doi:10.1016/j.rse.2013.03.031.
Li, L., L. Li, and K. Song (2015), Remote sensing of freshwater cyanobacteria: An extended IOP Inversion Model of Inland Waters (IIMIW) for partitioning absorption coefficient and estimating phycocyanin, *Remote Sens. Environ.*, *157*, 9–23, doi:10.1016/j.rse.2014.06.009.
Liu, X., Y. Zhang, M. Wang, and Y. Zhou (2014), High-frequency optical measurements in shallow Lake Taihu, China: Determining the relationships between hydrodynamic processes and inherent optical properties, *Hydrobiologia*, *724*(1), 187–201, doi:10.1007/s10750-013-1733-0.
Liu, Z., D. Hader, and R. Sommaruga (2004), Occurrence of mycosporine-like amino acids (MAAs) in the bloom-forming cyanobacterium *Microcystis aeruginosa*, *J. Plankton Res.*, *26*(8), 963–966, doi:10.1093/plankt/fbh083.
Llewellyn, C., J. Fishwick, and J. Blackford (2005), Phytoplankton community assemblage in the English Channel: A comparison using chlorophyll a derived from HPLC-CHEMTAX and carbon derived from microscopy cell counts, *J. Plankton Res.*, *27*(1), 103–119, doi:10.1093/plankt/fbh158.
Luis Perez, G., M. Eugenia Llames, L. Lagomarsino, and H. Zagarese (2011), Seasonal variability of optical properties in a highly turbid lake (Laguna Chascomus, Argentina), *Photochem. Photobiol.*, *87*(3), 659–670, doi:10.1111/j.1751-1097.2011.00907.x.
Martinez-Vicente, V., P. E. Land, G. H. Tilstone, C. Widdicombe, and J. R. Fishwick (2010), Particulate scattering and backscattering related to water constituents and seasonal changes in the Western English Channel, *J. Plankton Res.*, *32*(5), 603–619, doi:10.1093/plankt/fbq013.
Matthews, M. W., and S. Bernard (2013), Characterizing the absorption properties for remote sensing of three small optically-diverse South African reservoirs, *Remote Sens.*, *5*(9), 4370–4404, doi:10.3390/rs5094370.
Mckee, D., J. Piskozub, and I. Brown (2008), Scattering error corrections for in situ absorption and attenuation measurements, *Opt. Express*, *16*(24), 19,480–19,492, doi:10.1364/OE.16.019480.
Mishra, S., D. R. Mishra, Z. Lee, and C. S. Tucker (2013), Quantifying cyanobacterial phycocyanin concentration in turbid productive waters: A quasi-analytical approach, *Remote Sens. Environ.*, *133*, 141–151, doi:10.1016/j.rse.2013.02.004.
Mobley, C. D. (1994), *Light and Water: Radiative Transfer in Natural Waters*, Academic, San Diego, Calif.
Moran, M. A., and R. G. Zepp (1997), Role of photoreactions in the formation of biologically labile compounds from dissolved organic matter, *Limnol. Oceanogr.*, *42*(6), 1307–1316.
Morel, A., and B. Gentili (1991), Diffuse reflectance of oceanic waters—Its dependence on sun angle as influenced by the molecular-scattering contribution, *Appl. Opt.*, *30*(30), 4427–4438.
Morel, A., and S. Maritorena (2001), Bio-optical properties of oceanic waters: A reappraisal, *J. Geophys. Res.*, *106*(C4), 7163–7180, doi:10.1029/2000JC000319.
Morel, A., and L. Prieur (1977), Analysis of variations in ocean color, *Limnol. Oceanogr.*, *22*(4), 709–722.
Morel, A., B. Gentili, H. Claustre, M. Babin, A. Bricaud, J. Ras, and F. Tieche (2007), Optical properties of the "clearest" natural waters, *Limnol. Oceanogr. Methods*, *52*(1), 217–229.
Németh, J., and L. Vörös (1986), *Koncepció és Módszertan Felszíni Vizek Algológiai Monitoringjához*, Országos Környezet és Természetvédelmi Hivatal (OKTH), Budapest.
O'Donnell, D. M., S. W. Effler, C. M. Strait, and G. A. Leshkevich (2010), Optical characterizations and pursuit of optical closure for the western basin of Lake Erie through in situ measurements, *J. Great Lakes Res.*, *36*(4), 736–746, doi:10.1016/j.jglr.2010.08.009.
O'Donnell, D. M., S. W. Effler, M. Perkins, and C. Strait (2013), Optical characterization of Lake Champlain: Spatial heterogeneity and closure, *J. Great Lakes Res.*, *39*(2), 247–258, doi:10.1016/j.jglr.2013.03.004.
Palmer, S. C. J., T. Kutser, and P. D. Hunter (2015), Remote sensing of inland waters: Challenges, progress and future directions, *Remote Sens. Environ.*, *157*, 1–8, doi:10.1016/j.rse.2014.09.021.
Pegau, W., D. Gray, and J. Zaneveld (1997), Absorption and attenuation of visible and near-infrared light in water: Dependence on temperature and salinity, *Appl. Opt.*, *36*(24), 6035–6046, doi:10.1364/AO.36.006035.
Peng, F., and S. W. Effler (2013), Spectral absorption properties of mineral particles in western Lake Erie: Insights from individual particle analysis, *Limnol. Oceanogr. Methods*, *58*(5), 1775–1789, doi:10.4319/lo.2013.58.5.1775.
Perkins, M., S. W. Effler, C. Strait, and L. Zhang (2009), Light absorbing components in the Finger Lakes of New York, *Fundam. Appl. Limnol.*, *173*(4), 305–320, doi:10.1127/1863-9135/2009/0173-0305.
Perkins, M., S. W. Effler, F. Peng, D. M. O'Donnell, and C. Strait (2013), Light-absorbing components in the Great Lakes, *J. Great Lakes Res.*, *39*, 123–136, doi:10.1016/j.jglr.2013.04.003.
Perkins, M., S. W. Effler, and C. M. Strait (2014), Phytoplankton absorption and the chlorophyll a-specific absorption coefficient in dynamic Onondaga Lake, *Inland Waters*, *4*(2), 133–146, doi:10.5268/IW-4.2.607.
Présing, M., S. Herodek, L. Vörös, and I. Kobor (1996), Nitrogen fixation, ammonium and nitrate uptake during a bloom of *Cylindrospermopsis raciborskii* in Lake Balaton, *Arch. Hydrobiol.*, *136*(4), 553–562.
Présing, M., S. Herodek, T. Preston, and L. Vörös (2001), Nitrogen uptake and the importance of internal nitrogen loading in Lake Balaton, *Freshwater Biol.*, *46*(1), 125–139, doi:10.1046/j.1365-2427.2001.00622.x.
Prieur, L., and S. Sathyendranath (1981), An optical classification of coastal and oceanic waters based on the specific spectral absorption curves of phytoplankton pigments, dissolved organic-matter, and other particulate materials, *Limnol. Oceanogr.*, *26*(4), 671–689.
Sathyendranath, S., V. Stuart, B. D. Irwin, H. Maass, G. Savidge, L. Gilpin, and T. Platt (1999), Seasonal variations in bio-optical properties of phytoplankton in the Arabian Sea, *Deep Sea Res., Part II*, *46*(3–4), 633–653, doi:10.1016/S0967-0645(98)00121-0.
Shi, K., Y. Li, L. Li, and H. Lu (2013), Absorption characteristics of optically complex inland waters: Implications for water optical classification, *J. Geophys. Res. Biogeosci.*, *118*, 860–874, doi:10.1002/jgrg.20071.
Shiklomanov, I. (1993), World fresh water resources, in *Water in Crisis: A Guide to the World's Fresh Water Resources*, edited by P. H. Gleick, pp. 13–24, Oxford Univ. Press, N. Y.
Siegelman, H., and J. H. Kycia (1978), Algal biliproteins, in *Handbook of Phycological Methods*, edited by J. A. Hellebust and J. S. Craigie, pp. 71–79, Cambridge Univ. Press, N. Y.
Simis, S., S. Peters, and H. Gons (2005), Remote sensing of the cyanobacterial pigment phycocyanin in turbid inland water, *Limnol. Oceanogr. Methods*, *50*(1), 237–245.
Sinha, R. P., S. P. Singh, and D. Häder (2007), Database on mycosporines and mycosporine-like amino acids (MAAs) in fungi, cyanobacteria, macroalgae, phytoplankton and animals, *J. Photochem. Photobiol. B*, *89*(1), 29–35, doi:10.1016/j.jphotobiol.2007.07.006.
Slade, W. H., E. Boss, G. Dall'Olmo, M. R. Langner, J. Loftin, M. J. Behrenfeld, C. Roesler, and T. K. Westberry (2010), Underway and moored methods for improving accuracy in measurement of spectral particulate absorption and attenuation, *J. Atmos. Oceanic Technol.*, *27*(10), 1733–1746, doi:10.1175/2010JTECHO755.1.

Somlyódy, L., S. Herodek, C. Aradi, A. Clement, G. Dévai, V. Istvánovics, and G. Varga (1997), Revision of the Lower Kis-Balaton Reservoir, synthesis report no. 1, Tech. Univ., Budapest.

Sun, D., Y. Li, Q. Wang, H. Lv, C. Le, C. Huang, and S. Gong (2010), Partitioning particulate scattering and absorption into contributions of phytoplankton and non-algal particles in winter in Lake Taihu (China), *Hydrobiologia*, *644*(1), 337–349, doi:10.1007/s10750-010-0198-7.

Tassan, S., and G. Ferrari (1998), Measurement of light absorption by aquatic particles retained on filters: Determination of the optical pathlength amplification by the 'transmittance-reflectance' method, *J. Plankton Res.*, *20*(9), 1699–1709, doi:10.1093/plankt/20.9.1699.

Tilstone, G. H., G. F. Moore, K. Sorensen, R. Doerffer, R. Rottgers, K. G. Ruddick, R. Pasterkamp, and P. V. Jorgensen (2002), Regional validation of MERIS chlorophyll products in North Sea coastal waters, in *REVAMP Protocols, EVG1-CT-2001-00049*, pp. 1–77, Dev. of Generic Earth Observ. Technol., Paris.

Tilstone, G. H., T. Smyth, R. Gowen, V. Martinez-Vicente, and S. Groom (2005), Inherent optical properties of the Irish Sea and their effect on satellite primary production algorithms, *J. Plankton Res.*, *27*(11), 1127–1148, doi:10.1093/plankt/fbi075.

Tilstone, G. H., et al. (2012), Variability in specific-absorption properties and their use in a semi-analytical ocean colour algorithm for MERIS in North Sea and Western English Channel Coastal Waters, *Remote Sens. Environ.*, *118*, 320–338, doi:10.1016/j.rse.2011.11.019.

Twardowski, M., E. Boss, J. Sullivan, and P. Donaghay (2004), Modeling the spectral shape of absorption by chromophoric dissolved organic matter, *Mar. Chem.*, *89*(1–4), 69–88, doi:10.1016/j.marchem.2004.02.008.

Tyler, A., E. Svab, T. Preston, M. Présing, and A. W. Kovács (2006), Remote sensing of the water quality of shallow lakes: A mixture modelling approach to quantifying phytoplankton in water characterized by high-suspended sediment, *Int. J. Remote Sens.*, *27*(8), 1521–1537, doi:10.1080/01431160500419311.

Utermöhl, H. (1958), Zur Vervollkommnung der quantitativen Phytoplankton-Methodik, *Mitt. Int. Vereinigung Theor. Angew. Limnol.*, *9*, 1–38.

Verspecht, F., and C. Pattiaratchi (2010), On the significance of wind event frequency for particulate resuspension and light attenuation in coastal waters, *Cont. Shelf Res.*, *30*(18), 1971–1982, doi:10.1016/j.csr.2010.09.008.

Wang, Y., D. Liu, K. Song, J. Du, Z. Wang, B. Zhang, X. Tang, X. Lei, and Y. Wu (2011), Characterization of water constituents spectra absorption in Chagan Lake of Jilin Province, Northeast China, *Chin. Geogr. Sci.*, *21*(3), 334–345, doi:10.1007/s11769-011-0473-1.

Ylöstalo, P., K. Kallio, and J. Seppälä (2014), Absorption properties of in-water constituents and their variation among various lake types in the boreal region, *Remote Sens. Environ.*, *148*, 190–205, doi:10.1016/j.rse.2014.03.023.

Yoshimura, K., N. Zaitsu, Y. Sekimura, B. Matsushita, T. Fukushima, and A. Imai (2012), Parameterization of chlorophyll a-specific absorption coefficients and effects of their variations in a highly eutrophic lake: A case study at Lake Kasumigaura, Japan, *Hydrobiologia*, *691*(1), 157–169, doi:10.1007/s10750-012-1066-4.

Zaneveld, R., J. Kitchen, and C. Moore (1994), *The Scattering Error Correction of Reflecting-Tube Absorption Meters*, vol. 2258, SPIE—Int. Soc. Opt. Eng., Bellingham, Wash.

Zhang, Y., B. Qin, G. Zhu, G. Gao, L. Luo, and W. Chen (2006), Effect of sediment resuspension on underwater light field in shallow lakes in the middle and lower reaches of the Yangtze River: A case study in Longgan Lake and Taihu Lake, *Sci. China Ser. D*, *49*, 114–125, doi:10.1007/s11430-006-8111-y.

Zhang, Y., B. Qin, G. Zhu, L. Zhang, and L. Yang (2007), Chromophoric dissolved organic matter (CDOM) absorption characteristics in relation to fluorescence in Lake Taihu, China, a large shallow subtropical lake, *Hydrobiologia*, *581*(1), 43–52, doi:10.1007/s10750-006-0520-6.

Zhang, Y., L. Feng, J. Li, L. Luo, Y. Yin, M. Liu, and Y. Li (2010), Seasonal-spatial variation and remote sensing of phytoplankton absorption in Lake Taihu, a large eutrophic and shallow lake in China, *J. Plankton Res.*, *32*(7), 1023–1037, doi:10.1093/plankt/fbq039.

Zhang, Y., Y. Yin, X. Liu, Z. Shi, L. Feng, M. Liu, G. Zhu, Z. Gong, and B. Qin (2011), Spatial-seasonal dynamics of chromophoric dissolved organic matter in Lake Taihu, a large eutrophic, shallow lake in China, *Org. Geochem.*, *42*(5), 510–519, doi:10.1016/j.orggeochem.2011.03.007.

Zhang, Y., Y. Yin, M. Wang, and X. Liu (2012), Effect of phytoplankton community composition and cell size on absorption properties in eutrophic shallow lakes: Field and experimental evidence, *Opt. Express*, *20*(11), 11,882–11,898, doi:10.1364/OE.20.011882.